Published in final edited form as:

Nature. 2015 December 3; 528(7580): 132–136. doi:10.1038/nature16141.

A mechanism for expansion of regulatory T cell repertoire and its role in self tolerance

Yongqiang Feng[#1], **Joris van der Veeken**[#1], **Mikhail Shugay**[2,3], **Ekaterina V Putintseva**[2], **Hatice U Osmanbeyoglu**[4], **Stanislav Dikiy**[1], **Beatrice E Hoyos**[1], **Bruno Moltedo**[1], **Saskia Hemmers**[1], **Piper Treuting**[5], **Christina S Leslie**[4], **Dmitriy M Chudakov**[2,3], and **Alexander Y Rudensky**[1]

[1] Howard Hughes Medical Institute and Immunology Program, Ludwig Center at Memorial Sloan-Kettering Cancer Center, Memorial Sloan-Kettering Cancer Center, New York, NY 10065, USA.

[2] Shemyakin-Ovchinnikov Institute of Bioorganic Chemistry RAS, 117997, Miklukho-Maklaya 16/10, Moscow, Russia

[3] Pirogov Russian National Research Medical University, 117997, Ostrovityanova 1, Moscow, Russia

[4] Computational Biology Program, Memorial Sloan Kettering Cancer Center, New York, New York 10065, USA.

[5] Department of Comparative Medicine, School of Medicine, University of Washington, Seattle, Washington 98195, USA.

[#] These authors contributed equally to this work.

SUMMARY

T cell receptor (TCR) signaling plays a key role in T cell fate determination. Precursor cells expressing TCRs within a certain low affinity range for self peptide-MHC complexes undergo positive selection and differentiate into naïve T cells expressing a highly diverse self-MHC restricted TCR repertoire. In contrast, precursors displaying TCRs with a high affinity for "self" are either eliminated through TCR agonist induced apoptosis (negative selection)[1] or restrained by regulatory $CD4^+$ T (Treg) cells, whose differentiation and function are controlled by the X-chromosome encoded transcription factor Foxp3 (review[2]). Foxp3 is expressed in a fraction of self-reactive T cells that escape negative selection in response to agonist driven TCR signals combined with interleukin-2 (IL-2) receptor signaling. In addition to Treg cells, TCR agonist-

Correspondence and requests for materials should be addressed to A.Y.R. (; Email: rudenska@mskcc.org).

AUTHOR CONTRIBUTIONS

Y.F. and A.R. conceived and designed this study. Y.F. performed animal and *in vitro* studies, flow cytometric, TCR sequencing, and gene expression analyses. J.v.d.V. analyzed the epigenetic modifications of *CNS3* and their role in Foxp3 transcriptional regulation. M.S., E.V.P. and D.M.C. analyzed TCR sequencing data. H.U.O. and C.S.L. analyzed RNA sequencing data. B.E.H. performed serum Ig isotype analysis. S.D. and S.H. participated in phenotypic analysis of mice. S.H. generated Cre retroviral construct. B.M. and S.D. participated in optimizing TCR sequencing protocol. P.T. analyzed histopathology. Y.F. and A.Y.R. wrote the manuscript.

All RNA and TCR sequencing data have been deposited in the Gene Expression Omnibus under accession numbers GSE71309 and GSE71162 respectively. The authors declare no competing financial interests.

driven selection results in the generation of several other specialized T cell lineages like NKT and MAIT cells[3]. Although the latter exhibit a restricted TCR repertoire, Treg cells display a highly diverse collection of TCRs[4-6], Here we explored whether a specialized mechanism enables agonist driven selection of Treg cells with a diverse TCR repertoire and its significance for self-tolerance. We found that intronic *Foxp3* enhancer *CNS3* acts as an epigenetic switch that confers a poised state to the *Foxp3* promoter in precursor cells to make Treg cell lineage commitment responsive to a broad range of TCR stimuli, particularly to suboptimal ones. *CNS3*-dependent expansion of the TCR repertoire enables Treg cells to effectively control self-reactive T cells, especially when thymic negative selection was genetically impaired. Our findings highlight the complementary roles of these two main mechanisms of self-tolerance.

TCR signaling plays an essential role in Treg cell differentiation and function[7-10]. Recent studies have shown that a broad range of self-reactivity can promote Treg cell differentiation in the thymus, consistent with the highly diverse TCR repertoire of these cells[4-6]. We reasoned that a dedicated mechanism, linked to the regulation of *Foxp3* gene expression, might enable selection of Treg cells with a diverse TCR repertoire. Previously, we showed that an intronic element of the *Foxp3* gene, *CNS3,* increases the efficiency of Treg cell generation, raising the possibility that it might affect the composition of the Treg TCR repertoire. To account for the potential effects of a mixed 129/B6 genetic background in our previous study, we backcrossed the $Foxp3^{\Delta CNS3\text{-}gfp}$ allele onto a B6 genetic background and generated male $Foxp3^{\Delta CNS3\text{-}gfp}$ and $Foxp3^{gfp}$ littermates carrying identical N-terminal eGFP reporters[11,12]. Consistent with our previous observation[11], we found a ~40% reduction in $Foxp3^{+}CD4^{+}$ thymocytes in *CNS3*-deficient mice, compared to *CNS3*-sufficient littermate controls (2.05 ± 0.38% and 3.38 ± 0.70% of CD4 single-positive thymocytes respectively). The size of other thymocyte subsets was unaffected (Extended Data Fig. 1a, b). In contrast, peripheral Treg cells were present at comparable frequencies, most likely due to homeostatic expansion[7,13-15] (Extended Data Fig. 1a). Interestingly, *CNS3* deficiency had no effect on Foxp3 expression in differentiated Treg cells (Extended Data Fig. 1c). Our previous study suggested that *CNS3* is epigenetically marked in precursor cells, raising the question at which stage of T cell differentiation *CNS3* acts to facilitate Treg cell development. We found that ablation of a conditional *CNS3* allele in double positive (DP) or double-negative (DN) thymocytes using $Cd4^{Cre}$ or Lck^{Cre} drivers, respectively, resulted in similarly defective thymic Treg cell generation (Extended Data Fig. 1d, e). To assess the requirement for *CNS3* immediately preceding Foxp3 induction, we acutely ablated *CNS3* using tamoxifen-inducible Cre and observed decreased Foxp3 induction upon activation of naive $CD4^{+}$ T cells in the presence of TGF-β and IL-2 (Extended Data Fig. 1f). Interestingly, in mature Treg cells *CNS3* was fully dispensable for the maintenance of Foxp3 expression during cell division in the presence of pro-inflammatory cytokines (Extended Data Fig. 1g, h), and for their suppressor function *in vivo* (Extended Data Fig. 2).

These findings raised the question of how, mechanistically, *CNS3* could selectively facilitate the initiation, but not the maintenance of Foxp3 expression. To begin addressing this problem, we sought to identify the stage of thymocyte differentiation at which the *CNS3* region first acquires features characteristic of a poised enhancer. We previously found that *CNS3* is marked by lysine 4 monomethylation of histone H3 (H4K4me1) in DP

thymocytes[11]. Unexpectedly, we found increased H3K4me1 at *CNS3* at DN1 stage and in hematopoietic stem cells (HSC), comparable to the levels observed in DP, CD4 SP thymocytes, and naïve $CD4^+$ and $CD8^+$ T cells (Fig. 1a-c and data not shown). In contrast, *CNS3* chromatin was not enriched for H3K4me1 in embryonic stem cells (ESC), macrophages (Mφ), or dendritic cells (DC) (Fig. 1b, c). These results indicate that the poised state of *CNS3* is established at a very early stage of hematopoiesis, but is lost in "non-T" cell lineages. Because *CNS3* appeared to be the earliest epigenetically modified region in the *Foxp3* locus, it might exert its function by facilitating chromatin remodeling at the *Foxp3* promoter.

While deposition of the "active" histone modifications H3K4me3 and H3K27Ac at the *Foxp3* promoter occurred exclusively in Treg cells (Extended Data Fig. 3a, b), we found an enrichment of H3K4me1 in mature CD4 SP thymocytes and naïve $CD4^+$ T cells (Fig 1d). In the absence of *CNS3*, both mature CD4 SP thymocytes and naïve $CD4^+$ T cells showed impaired H3K4me1 accumulation at the *Foxp3* promoter (Fig. 1e, f), suggesting that *CNS3* facilitates epigenetic remodeling of the *Foxp3* promoter in Treg precursors. Interestingly, differentiated *CNS3*-deficient Treg cells showed normal levels of H3K4me3 and H3K27Ac deposition at the *Foxp3* regulatory regions (Extended Data Fig. 3c-e), consistent with the dispensable role of *CNS3* in differentiated Treg cells (Extended Data Fig. 1c, g, h).

To address whether the *CNS3*-dependent poised state of the *Foxp3* promoter assists deposition of additional permissive marks and further chromatin remodeling that facilitates the initiation of Foxp3 expression, we cultured naive $CD4^+$ T cells from male $Foxp3^{gfp}$ and $Foxp3^{\Delta CNS3\text{-}gfp}$ littermates under Treg cell differentiation conditions and isolated $Foxp3^-$ cells that had been exposed to Foxp3-inducing conditions, but did not yet acquire Foxp3 expression. We observed a *CNS3*-dependent increase in H3K27Ac at the *Foxp3* promoter preceding Foxp3 expression (Extended Data Fig. 3f), consistent with the defect in Treg cell differentiation in the absence of *CNS3* (Extended Data Fig 1f). As a proof, blocking the recruitment of bromodomain-containing histone acetylation readers using iBET sharply reduced Treg cell induction efficiency in a dose-dependent manner (Extended Data Fig. 3g)[16]. Conversely, blocking histone deacetylase (HDAC) activity using butyrate increased H3K27Ac at the *Foxp3* promoter in agreement with recent reports[17-19] (Fig. 1g). Importantly, provision of butyrate rescued impaired *in vitro* Treg cell differentiation associated with *CNS3* deficiency (Fig. 1h). These observations suggest that a *CNS3*-dependent poised state at the *Foxp3* promoter, likely via looping, in precursor cells may enhance their sensitivity to Foxp3-inducing signals (Extended Data Fig. 3h).

While *CNS3*-dependent poising of the *Foxp3* promoter could facilitate Foxp3 induction in a probabilistic manner, it might also enable lower strength TCR signals to promote Treg cell differentiation. To address this possibility we tested whether impaired Foxp3 induction in *CNS3*-deficient naïve $CD4^+$ T cells could be rescued by increasing amounts of CD3 antibody under *in vitro* Treg cell differentiation conditions. We found that the relative difference in the efficiency of Foxp3 induction between *CNS3*-sufficient and - deficient $CD4^+$ T cells was markedly decreased in the presence of higher amounts of CD3 antibody (Fig. 2a and Extended Data Fig. 4a), suggesting that increased TCR signal strength can partially compensate for the lack of *Foxp3* promoter poising in the absence of *CNS3,* and

imply that differentiation of Treg precursors receiving lower TCR stimulation might be disproportionally impeded by *CNS3* deficiency. A corollary of this notion is that the mature Treg cells differentiated from *CNS3*-deficient precursors are enriched for TCRs at the higher end of the self-reactivity spectrum, and depleted of those with lower self-reactivity.

To test this possibility we analyzed Foxp3^{-} and Foxp3^{+} CD4 SP thymocytes and naïve CD4^{+} T cells for the expression of orphan nuclear receptor Nr4a1 (Nur77), a prominent TCR target gene in Treg and conventional T cells that accurately reports the strength of TCR signaling[20,21]. In agreement with the *in vitro* Foxp3 induction studies, we found that both thymic and peripheral *CNS3*-deficient Treg, but not Foxp3^{-}CD4^{+} T cells were markedly enriched for cells expressing higher levels of Nur77 in comparison to their *CNS3*-sufficient counterparts. This trend was observed in non-competitive settings of male *Foxp3^{gfp}* and *Foxp3$^{\Delta CNS3\text{-}gfp}$* littermates, as well as in competitive settings, upon ablation of *CNS3* in bone marrow chimeras and in heterozygous female *Foxp3$^{gfp/+}$* and *Foxp3$^{\Delta CNS3\text{-}gfp/+}$* littermates (Fig. 2b, Extended Data Fig. 4b-d, and data not shown). Notably, Nur77 levels were increased in both resting (CD62L^{hi}CD44^{lo}) and activated (CD62L^{lo}CD44^{hi}) *CNS3*-deficient Treg cells (Extended Data Fig. 4e-g). In contrast, its expression in Foxp3^{-} thymocytes and peripheral T cells was unaffected in the absence of *CNS3* (Extended Data Fig. 4d). Consistently, *CNS3*-deficient Treg cells expressed increased amounts of CTLA4, a major negative feedback regulator of TCR signaling, and cell proliferation marker Ki67 (Extended Data Fig. 4h, i). Finally, we found that *CNS3*-deficient and -sufficient Foxp3^{+} CD4 SP thymocytes and resting peripheral Treg cells exhibited distinct gene expression profiles, in contrast to Foxp3^{-} subsets (Extended Data Fig. 5a). Specifically, expression of TCR-dependent genes and genes characteristic of activated Treg cells was significantly increased in *CNS3*-deficient Foxp3^{+} thymocytes and resting Treg cells in comparison to their *CNS3*-sufficient counterparts (Fig. 2c, d and Extended Data Fig. 5b, d). In contrast, transcriptional profiles of *CNS3*-sufficient and -deficient activated Treg cells and Foxp3^{-} CD4 SP thymocytes were similar (Extended Data Fig. 5a, c, e and data not shown). These results further supported the notion that *CNS3* deficiency resulted in an enrichment for thymic Treg cells with a heightened TCR signal strength.

To assess the autoreactivity of *CNS3*-deficient vs. -sufficient Treg cells *in vivo*, we examined their capacity for MHC class II (MHC-II) dependent homeostatic expansion under lymphopenic conditions, known to be proportional to TCR affinity for "self"[5]. *CNS3*-deficient Treg cells expanded markedly more than *CNS3*-sufficient counterparts, upon co-transfer with congenically labeled effector T cells into lymphopenic hosts (*Tcrb$^{-/-}$Tcrd$^{-/-}$*), which was likely driven by the recognition of self-antigens presented by MHC-II molecules, because antibody mediated blockage of MHC-II prevented expansion Treg cells and erased the advantage of *CNS3*-deficient Treg cells over their *CNS3*-sufficient counterparts (Fig. 2e, f, Extended Data Fig. 5f). Accordingly, the frequency of *CNS3*-deficient Treg cells was noticeably increased in the periphery of *Foxp3$^{\Delta CNS3\text{-}gfp/+}$* compared to *Foxp3$^{gfp/+}$* heterozygous females (Extended Data Fig. 5g). Thus, Treg cells developed from precursors lacking *CNS3* resulted in a skewed TCR repertoire.

We next examined the TCR repertoires of Treg cells, naïve and activated CD4^{+} T cells in *Foxp3$^{\Delta CNS3\text{-}gfp}$* or *Foxp3^{gfp} Tcra$^{-/+}$* mice expressing the DO11.10 TCRβ chain transgene

where TCR diversity is limited to a single functional TCRα chain locus[5]. Barcoded TCRα libraries were generated using an optimized protocol and high throughput sequencing data were analyzed using MIGEC software package[22]. Cluster analysis using VDJtools[23] showed that TCRα repertoires of thymic and peripheral *CNS3*-deficient and -sufficient Treg, but not naïve or activated effector CD4$^+$ T cells were distinct (Fig. 2g). Further analysis showed a significantly reduced TCRα diversity of *CNS3*-deficient Treg, but not naïve or effector CD4$^+$ T cells in comparison to their *CNS3*-sufficient counterparts (Fig. 2h). Since the TCR Complementarity-Determining Region 3 (CDR3) largely determines TCR specificity for peptide-MHC complexes (pMHC), we assessed the frequencies of strongly interacting amino acid residues in TCRα CDR3 by leveraging a mathematical model linking the features of amino acid residues in the CDR3 to TCR affinity for pMHC[24]. Interestingly, the TCRα CDR3s were significantly enriched for strongly interacting amino acid residues (Extended Data Fig. 5h, i), and for more randomly added nucleotides (Supplementary Table 1) in *CNS3*-deficient vs. -sufficient Treg, but not naïve or effector CD4$^+$ T cells. These results implied higher affinities of *CNS3*-deficient Treg TCRs for self-antigens and further supported the notion that *CNS3* shapes Treg TCR repertoire by increasing its diversity, likely, by enabling Treg differentiation in response to a broad range of self-reactivity.

To understand the functional significance of *CNS3*-dependent regulation of the Treg cell repertoire, we first assessed the immune status of male *Foxp3*$^{\Delta CNS3\text{-}gfp}$ and their wild type *Foxp3*^{gfp} littermates. We observed no effect of *CNS3* deficiency on the numbers of activated or memory CD4$^+$ or CD8$^+$ T cells and on cytokine production by T cells in the secondary lymphoid organs in 8-12 week old mice (Fig. 3a-c and data not shown). Although *CNS3*-deficient Treg cells were capable of preventing systemic autoimmunity (Fig. 3a-c, Extended Data Fig. 1a), it remained possible that the skewed Treg TCR repertoire might have “holes”. Thus, we reasoned that select few non-lymphoid organs may exhibit focused immune activation in *CNS3*-deficient vs. *CNS3*-sufficient mice, whereas others might be similarly or even more protected against autoimmunity by the overrepresented highly autoreactive Treg cells. Indeed, we found increased numbers of activated effector T cells and elevated IL-13 and IFNγ production by T cells in the lungs of *Foxp3*$^{\Delta CNS3\text{-}gfp}$ mice (Fig. 3a-c). We also observed markedly elevated titers of circulating autoantibodies against a number of self-antigens in the sera of *CNS3*-deficient mice vs. their wild-type *Foxp3*^{gfp} littermates, whereas the absolute amounts of Ig isotypes were comparable (Fig. 3d, Extended Data Fig. 6a and data not shown). This notion was further supported by the observed modest, but consistent, decrease in the severity of experimental autoimmune encephalomyelitis (EAE) in *Foxp3*$^{\Delta CNS3\text{-}gfp}$ vs. *Foxp3*^{gfp} littermates (Extended Data Fig. 6b-f). To directly compare the suppressive capacity of Treg cells developed in *CNS3*-deficient and -sufficient mice, we transferred these Ly5.2$^+$ Treg cells together with Ly5.1$^+$ *Foxp3*^{null} (*ΔFoxp3*) effector T cells into T cell-deficient recipients (Fig. 3e). Despite comparable expansion of *CNS3*-sufficient and -deficient Treg cells in the recipients, we observed more pronounced weight loss and increased pro-inflammatory cytokine production by effector *ΔFoxp3* T cells in the presence of *CNS3*-deficient Treg cells in comparison to the control (Fig. 3f-h and Extended Data Fig. 6g, h). These results indicate that Treg cells developed from *CNS3*-deficient precursors were selectively impaired in their capacity to suppress self-reactive effector T cells.

Both negative selection and Treg cell generation are driven by self-antigen recognition in the thymus and likely play complementary roles in self-tolerance[1,2,25,26]. We reasoned that the relatively mild impairment in suppressive capacity of Treg cells from *CNS3*-deficient mice on a B6 genetic background, resistant to autoimmunity, may not fully reveal the biological significance of *CNS3*-dependent broadening of the Treg cell repertoire because of efficient negative selection. Therefore, we assessed the consequences of combined deficiency in *CNS3* and *Aire* (*Autoimmune Regulator*), a nuclear factor required for thymic negative selection and optimal Treg cell generation. *Aire* deficiency leads to diminished expression of a subset of tissue-restricted antigens in the thymus and, consequently, an enlarged self-reactive effector T cell pool and diminished Treg repertoire[25,27–29]. In contrast to a late-onset and rather mild autoimmunity observed in *Aire* deficient mice on a B6 genetic background, double deficiency in *CNS3* and *Aire* resulted in fatal early-onset aggressive autoimmune lesions in multiple tissues as early as 3-4 weeks of age, when detectable autoimmune inflammation was lacking in littermates with a single deficiency in *Aire* or *CNS3* (Fig. 4a and Extended Data Fig. 7a). We noticed a 100% (n>35) penetrance with a stochastic gender independent variation in manifestations expected from perturbations in randomly generated repertoires of self-reactive T cells as well as the probabilistic nature of negative selection[30] (Extended Data Fig. 7a and data not shown). This was accompanied by significant increases in $CD4^+$ T cell activation, IFNγ production (Fig. 4b, c), serum Ig levels (Extended Data Fig. 7b), and autoantibody production (Fig. 4d). Combined *Aire* and *CNS3* deficiency resulted in a further reduction in thymic Treg cell frequency in comparison to the single deficient mice (1.66 ± 0.28% and 0.91 ± 0.35% in $Foxp3^{\Delta CNS3\text{-}gfp}$ $Aire^{KO/WT}$ and $Foxp3^{\Delta CNS3\text{-}gfp}$ $Aire^{KO/KO}$ mice, respectively)[25] (Fig. 4e). However, peripheral Treg cells reached normal levels in young $Foxp3^{\Delta CNS3\text{-}gfp}Aire^{KO/KO}$ mice prior to development of clinical signs of disease likely due to homeostatic proliferation (Fig. 4f). Despite their normal quantities and Foxp3 expression, these Treg cells were unable to suppress pathogenic self-reactive T cells resulting from impaired negative selection in the absence of *Aire* (Fig.4b-d, Extended Data Fig. 7c). Since diminished thymic Treg cell numbers and their skewed TCR repertoire likely contributed to disease severity in $Foxp3^{\Delta CNS3\text{-}gfp}Aire^{KO/KO}$ mice, we directly assessed the ability of *CNS3*-sufficient and -deficient Treg cells developed in the presence of *Aire* to control $Foxp3^{\Delta CNS3\text{-}gfp}Aire^{KO/KO}$ effector T cells when adoptively transferred into T cell deficient hosts. Although the negative impact of *CNS3* deficiency on the TCR repertoire was likely mitigated by Treg cell expansion in lymphopenic settings, *CNS3*-deficient Treg cells still exhibited compromised ability to suppress the responses of transferred $Foxp3^{\Delta CNS3\text{-}gfp}Aire^{KO/KO}$ effector T cells and resident B cells in comparison to the controls (Extended Data Fig. 7d-i). These results suggest that control of broad self-reactive T cells requires a diverse *CNS3*-dependent repertoire of Treg cells.

Our studies suggest that *CNS3*, an intronic *Foxp3* regulatory element, establishes a poised state of the *Foxp3* promoter in precursor cells and increases the probability of Foxp3 induction in response to TCR stimulation, particularly, within a lower range of signal strength (Extended Data Fig. 8). Similar mechanisms of promoter poising may operate in other cell types and enable them to respond to a wider spectrum of growth factor or morphogen concentrations through receptor-triggered analogue signaling. *CNS3* mediated

Foxp3 promoter poising expands the TCR repertoire of Treg cells, which is essential for keeping pathogenic self-reactive T cells that escape negative selection in check.

METHODS

Mice

Foxp3$^{CNS3\text{-}fl\text{-}gfp}$ mice were generated using ES cell line CY2.4 (C56BL/6) as previously described[11]. *Cd4*^{Cre}, *Lck*^{Cre}, *UBC*$^{Cre\text{-}ERT2}$ and Rosa26-stop-YFP (R26Y) mice were obtained from the Jackson Laboratories. DO11.10 TCRβ transgenic and *Aire* knockout mice were kindly provided by Philippa Marrack, Diane Mathis and Christophe Benoist, respectively. Heterozygous females carrying *Foxp3*$^{\Delta CNS3\text{-}gfp}$ and *Foxp3*^{gfp} were crossed with B6 males to generate hemizygous *Foxp3*$^{\Delta CNS3\text{-}gfp}$ and wild type *Foxp3*^{gfp} littermates. *Rag1*$^{-/-}$, CD45.1 *Foxp3*^{gfp} and *Tcrb*$^{-/-}$*Tcrd*$^{-/-}$ mice were maintained in our animal facility. To study the genetic interactions between *CNS3* and *Aire*, heterozygous females of *Foxp3*$^{\Delta CNS3\text{-}gfp/gfp}$ were first crossed with *Aire*$^{KO/WT}$, and F1 harboring *Aire*$^{KO/WT}$ and *Foxp3*$^{\Delta CNS3\text{-}gfp}$ or *Foxp3*^{gfp} were then intercrossed to generate *Aire*$^{KO/KO}$ or *Aire*$^{KO/WT}$ mice carrying *Foxp3*$^{\Delta CNS3\text{-}gfp}$ or *Foxp3*^{gfp}. To examine TCR diversity with restricted repertoire, *Foxp3*$^{\Delta CNS3\text{-}gfp/gfp}$ heterozygous females were crossed to the DO11.10 TCRβ transgenic and *Tcra*$^{-/+}$ males. F1 males of *Foxp3*$^{\Delta CNS3\text{-}gfp}$ or *Foxp3*^{gfp} mice carrying the DO11.10 TCRβ transgene and *Tcra*$^{-/+}$ were used for T cell isolation and TCR sequencing. To induce deletion of *CNS3 in vivo*, tamoxifen solution (40mg/ml in olive oil) was administered by gavage to *UBC*$^{Cre\text{-}ERT2}$ R26Y *Foxp3*$^{CNS3fl\text{-}gfp}$ mice more than 3 days before lymphocyte isolation.

All mice were maintained in the MSKCC animal facility under SPF conditions, and the experiments were approved by the institutional review board (IACUC 08-10-023).

Statistical Analysis

Statistical tests were performed with Prism (GraphPad), Excel (Microsoft), or R statistical environment. Box-and-whisker plots show minimum, maximum, first and third quartiles and median.

Cell culture

For *in vitro* Treg cell differentiation, naïve CD4$^+$ T cells (GFP$^-$CD25$^-$CD44^{lo}CD62L^{hi}) or mature CD4$^+$CD8$^-$ single positive (TCRβ^{hi}GFP$^-$CD25$^-$CD69^{lo}CD62L^{hi}) T cells were sorted from *Foxp3*^{gfp}, *Foxp3*$^{\Delta CNS3\text{-}gfp}$ or *Foxp3*$^{CNS3fl\text{-}gfp}$ mice after the enrichment of CD4$^+$ T cells or depletion of CD8$^+$ T cells using Dynabeads FlowComp Mouse CD4 or CD8 kits respectively (Life Technologies), and then cultured with lethally irradiated (20Gy) antigen presentation cells (splenocytes depleted of T cells with Dynabeads FlowComp Mouse CD90.2 kit, Life Technologies) or on plates pre-coated with CD3 and CD28 antibodies in RPMI1640 supplemented with 10% fetal bovine serum (FBS), 2mM L-glutamine, 1mM sodium pyruvate, 10mM HEPES, 2×10^{-5} M 2-mercaptoethanol, 100 U/ml penicillin, 100 mg/ml streptomycin, and 500 U/ml IL-2 and 1ng/ml TGFβ. Sodium butyrate (water solution) or iBET solution in DMSO (a kind gift from R. Prinha) were added to the culture to block HDAC or bromodomain containing proteins respectively. Treg cells were sorted

based on *Foxp3*^{gfp} reporter expression. Assessment of the stability of Foxp3 expression *in vitro* was performed as previously described[31]. Briefly, Treg cells were activated upon culture in the presence of CD3 and CD28 antibody-coated beads (Life Technologies) with the following recombinant pro-inflammatory cytokines: IL-2 (250U/ml), IL-4 (20 ng/ml), IL-6 (10ng/ml), and IFNγ (100 ng/ml), IL-12 (20ng/ml).

In vivo suppression assay

To assess Treg cell suppressor capacity *in vivo* we conducted adoptive T cell transfers into T cell deficient recipients as previously described[31]. Briefly, 2.5~3.0×10^6 Foxp3$^-$ CD4$^+$ and/or CD8$^+$ T cells isolated from *Foxp3*^{gfpko} or *Foxp3*$^{\Delta CNS3\text{-}gfp}$ *Aire*$^{KO/KO}$ mice were transferred to congenic and gender matched *Tcrb*$^{-/-}$ *Tcrd*$^{-/-}$ recipients alone or at 10:1 ratio with sorted Treg cells from *Foxp3*^{gfp} or *Foxp3*$^{\Delta CNS3\text{-}gfp}$ littermates. Similar numbers of effector T cells and Treg cells were used for *in vivo* evaluation of Treg suppressor function after acute ablation of *CNS3*. Recipient mice were monitored for body weight change regularly and lymphocytes were analyzed by flow cytometry at least 4 weeks after the transfer.

Treg cell homeostatic proliferation in lymphopenic mice

8-10 weeks after bone marrow reconstitution of CD45.1 *Foxp3*^{gfp} and CD45.2 *Foxp3*$^{\Delta CNS3\text{-}gfp}$ in *Tcrb*$^{-/-}$*Tcrd*$^{-/-}$ recipients, CD45.1$^+$ and CD45.2$^+$ Treg cells (CD4$^+$GFP$^+$) were sorted, mixed at a 1:1 ratio and co-transferred into *Tcrb*$^{-/-}$*Tcrd*$^{-/-}$ male mice with 10 fold naïve CD4$^+$ T cells (CD25$^-$CD44^{lo}CD62L^{hi}) isolated from wild type CD45.2 B6 males. To block TCR stimulation by self peptide-MHC class II complexes, 0.5 mg I-A^b specific monoclonal antibody Y3P (IgG2a) or control IgG2a (Bio X Cell) was injected i.v. every other day before and after T cell transfer[32,33]. The lymphocyte subsets were analyzed by flow cytometry 9 days later.

Flow cytometric analyses and tissue lymphocyte preparation

Tissue lymphocytes were prepared as previously described[31]. The following fluorophore-conjugated antibodies were used for cell surface staining: CD4 (RM4-5, eBioscience), CD8 (5H10, Life Technologies), CD25 (PC61.5, eBioscience), CD3e (145-2C11, eBioscience), CD44 (IM7, eBioscience), CD62L (MEL-14, eBioscience), CTLA4 (UC10-4B9, eBioscience), TCRβ (BioLegend), CD45.1 (A20, eBioscience), CD45.2 (104, eBioscience). Antibodies used for intracellular staining: Foxp3 (FJK-16s, eBioscience), Ki67 (B56, BD Biosciences), IL-17 (eBio17B7, eBioscience), IFNγ (XMG1.2, eBioscience), IL-2 (JES6-5H4, eBioscience). To stain endogenous Nur77, cells were incubated with rabbit-anti-Nur77 antibody (Cell Signaling) after fixation and permeabilization with Foxp3/ transcription factor staining buffer set (eBioscience) followed by phycoerythrin (PE) conjugated donkey-anti-rabbit antibody (eBioscience). For the flow cytometric analysis of cytokine production, lymphocytes were first stimulated *in vitro* with 10mg/ml of CD3 antibody in the presence of monensin (BD Biosciences) at 37°C for 5 hours, then stained with antibodies against indicated cell surface markers followed by staining of cytokines with intracellular staining kit (BD Biosciences). All flow cytometric analyses were performed using live cell gate defined as negative by staining with the LIVE/DEAD Fixable Dead Cell Stain Kit (Life Technologies). Flow cytometric analysis was performed with FlowJo (Treestar).

Retroviral transduction

Cre coding region was subcloned into MigR1-IRES-Thy1.1 vector (A. Levine, unpublished) to generate MigR1-Cre-IRES-Thy1.1. Retroviral packaging with regular Phoenix-ECO cells and transduction of Treg cells were performed with standard protocols[5].

Autoantibody profiling using Autoantigen Microarrays

Analysis of autoantibody reactivity against a panel of 95 auto-antigens was conducted using the autoantigen microarrays developed by University of Texas Southwestern Medical Center[34]. Briefly, serum samples pretreated with DNase-I and diluted at 1:50 were incubated with the autoantigen arrays. After a second incubation with Cy3-conjugated anti-mouse IgG the arrays were scanned with a Genepix 4200A scanner (Molecular Device). The fluorescent signals for individual auto-antigens were extracted from the resulting images with Genepix Pro 6.0 (Molecular Devices), followed sequentially by subtraction of local background, average of duplicates, normalization with total IgG, and subtraction of a negative PBS control.

TCR sequencing and data analysis

Cell isolation and RNA extraction—Lymphocytes harvested from the peripheral lymphoid organs or thymi of 6-8 week old male *Foxp3*^{gfp} or *Foxp3*$^{\Delta CNS3\text{-}gfp}$ *Tcra*$^{-/+}$ littermates bearing the DO11.10 TCRβ transgene and were enriched for CD4^{+} T cells (Dynabeads FlowComp Mouse CD4 kit, Life Technologies) or depleted of CD8^{+} T cells (Dynabeads FlowComp Mouse CD8 kit, Life Technologies), respectively, and Treg cells (CD4^{+}GFP^{+}), mature Foxp3^{-}CD4 single positive thymocytes (CD4^{+}CD8^{-}GFP^{-}CD25^{-}CD69^{lo}CD62L^{hi}), peripheral naïve (CD4^{+}GFP^{-}CD25^{-}CD44^{lo}CD62L^{hi}) and effector CD4 T cells (CD4^{+}GFP^{-}CD44^{hi}CD62L^{lo}) were isolated using a FACSAria II sorter (BD) gated on TCR-Vβ8^{hi}. Total RNA from TRIzol preserved cell lysates was performed according to the manufacturer's manual (Life Technologies). mRNA was purified from total RNA with Dynabeads mRNA DIRECT Kit (Life Technologies) and used for reverse transcription.

cDNA synthesis—In order to maximize the priming efficiency of reverse transcription (RT), a mixture of oligo(dT)$_{24}$ and eight DNA oligonucleotides corresponding to mouse TCRα constant region was used. The oligonucleotides used in this study were synthesized by Integrated DNA Technologies, Inc. TRAC_RT1: CTCAGCGTCATGAGCAGGTTAAAT,

TRAC_RT2: CAGGAGGATTCGGAGTCCCATAA,

TRAC_RT3: TTTTACAACATTCTCCAAGA,

TRAC_RT4: TTCTGAATCACCTTTAATGA,

TRAC_RT5: ATGAGATAATTTCTACACCT,

TRAC_RT6: TTTGGCTTGAAGAAGGAGCG,

TRAC_RT7: TTCAAAGCTTTTCTCAGTCA,

TRAC_RT9: TGGTCTCTTTGAAGATATCT.

To label the 5'end of TCRα mRNA, a DNA-RNA hybrid oligonucleotide with 12 random nucleotides serving as barcodes to tag individual mRNA molecules was synthesized as reported[35].

Hybrid oligo: AAGCAGTGGTATCAACGCAGAGUNNNNUNNNNUNNNNUCTTrGrGrGrGrG (r, ribonucleotide). cDNA was synthesized in SMARTScribe reverse transcription buffer (Clontech) with 1.0μM each RT oligo, 0.5mM each dNTP, 5.0mM DTT, 2.0U/μl recombinant ribonuclease inhibitor (Takara), 1μM hybrid oligo, 1M betaine (Affymetrix), 6mM $MgCl_2$, and 5U/μl SMARTScribe Reverse Transcriptase by incubating at 42°C for 90 minutes followed by 10 cycles of incubation at 50°C for 2 minutes and 42°C for 2 minutes, and one step of incubation at 70°C for 15 min. After removal of hybrid oligo with Uracil-DNA Glycosylase (New England BioLabs) cDNA was purified with Agencourt AMPure XP beads (Beckman Coulter) according the manufacturer's manual.

Sequencing library preparation—Purified cDNA was used as templates for a four-step PCR amplification, in which sequencing adaptors and sample indices were introduced. The first PCR reaction was performed with purified cDNA, 0.2μM universal primer (CTAATACGACTCACTATAGGGCAAGCAGTGGTATCAACGCAGAGT, Clontech), 0.2μM TRAC reverse primer 8 (TTTTGTCAGTGATGAACGTT), 0.2mM each dNTP, 1.5mM $MgCl_2$, 0.02U/μl KOD Hot Start DNA Polymerase (EMD Millipore). PCR parameters were as the follows: initial denature at 95°C for 2 minutes; 10 cycles of 95°C 20 seconds, 70°C 10 seconds with an increment of −1°C per cycle, and 70°C 30 seconds; 15 cycles of 95°C 20 seconds, 60°C 10 seconds and 70°C 30 seconds; final 70°C 3.5 minutes. Amplified DNA was purified with Agencourt AMPure XP magnetic beads for the subsequent reaction. The second PCR reaction used the same ingredients except that the reverse primer was replaced by a nested primer (CAATTGCACCCTTACCACGACAGT CTGGTACACAGCAGGTTCTGGGTTCTGGA). Cycling parameters are: 95°C for 2 minutes; 6 cycles of 95°C 20 seconds, 60°C 10 seconds and 70°C 30 seconds; final 70°C 3.5 minutes. DNA from individual samples was extracted with Agencourt AMPure XP magnetic beads and used for the third round of amplification with 5RACE TCR forward primer (AATGATACGGCGACCACCGAGATCTACACCTAATACGACTCACTATAGGGC) and indexed reverse primer (CAAGCAGAAGACGGCATACGAGATXXXXXXAGTCAGTCAG CC CAATTGCACCCTTACCACGA, XXXXXX for 6-nucleotide barcode). Cycling parameters are: 95°C for 2 minutes; 6 cycles of 95°C 20 seconds, 55°C 10 seconds and 70°C 30 seconds; 70°C 3.5 minutes. PCR reaction was purified with Agencourt AMPure XP magnetic beads and used for the fourth PCR amplification with primers P1 (AATGATACGGCGACCACCGAG) and P2 (CAAGCAGAAGACGGCATACGA), and the following cycling parameters: 95°C for 2 minutes; 5 cycles of 95°C 20 seconds, 57°C 10 seconds and 70°C 30 seconds; 70°C 3.5 minutes. The final PCR products were separated by agarose gel electrophoresis and a single band around 600 base pairs was cut and extracted with Gel Extraction and PCR Clean-Up kits (Takara).

High-throughput sequencing—Samples were quantified with Kapa Library Quantification kits (Kapa Biosystems) and sequenced on a MiSeq sequencer (Illumina) using 200 cycles of read 1, 6 cycles of index read and 200 cycles of read 2 with the following customized primers:

Read 1: CTAATACGACTCACTATAGGGCAAGCAGTGGTATCAACGCAGAGT.

Index read: TCGTGGTAAGGGTGCAATTGGGCTGACTGACT.

Read 2: AGTCAGTCAGCCCAATTGCACCCTTACCACGA.

Data analysis—Barcoded sequencing data were analyzed with MIGEC software[22]. Briefly, unique molecular identifier (UMI) sequences were extracted from raw sequencing data (Read 1) with MIGEC/Checkout routine. Reads (≥5) bearing the same UMI were grouped and assembled to generate consensus sequences with MIGEC/Assemble. Variable (V) and Joining (J) segment mapping, Complementarity Determining Region 3 (CDR3) extraction, and error correction were performed with MIGEC/CdrBlast as previously described[22], which eliminates PCR and sequencing errors, as well as normalizes the output data as cDNA counts that represent the TCR clonotypes in a population[36].

Comparison of TCRα repertoires between *CNS3*-deficient and -sufficient mice at protein level was evaluated using VDJtools post-analysis framework (https://github.com/mikessh/vdjtools)[23]. Pearson correlation of clonotype frequencies for the shared TCR clones was used for the generation of the dendrogram. Clonal diversities of TCRα repertoires were evaluated using inverse Simpson index computed separately for individual samples after downsampling the repertoires to the size of the smallest sample from the same organ. Similar downsampling strategy, not weighted by clonotype frequencies, was used to compute the average size of added nucleotides in CDR3. A mathematical model proposed by Kosmrlj et al.[24] was used to assess the strength of CDR3 amino-acid interactions with self-peptide-MHC complexes. Numbers of strongly interacting amino acid residues (LFIMVWCY) were calculated for the V-segment part of TCRα CDR3 and V-J segment junction. Those numbers were then weighted by the corresponding clonotype frequencies and the resulting sums were used for the comparisons between samples.

RNA sequencing and data analysis

Mature Foxp3^{-} CD4^{+}CD8^{-} single positive (TCRβ^{+}GFP^{-}CD62L^{hi}CD69^{lo}) thymocytes, Foxp3^{+} CD4 SP thymocytes (thymic Treg cells), peripheral resting (CD44^{lo}CD62L^{hi}) and activated (CD44^{hi}CD62L^{lo}) Treg cells were FACS sorted from 6~8 week old male *Foxp3^{gfp}* and *Foxp3$^{\Delta CNS3\text{-}gfp}$* littermates. RNA was extracted and cDNA libraries were generated after SMART amplification (Clontech). Libraries were sequenced using a HiSeq 2000 platform (Illumina) according to a standard paired-end protocol. Reads were first processed with Trimmomatic[37] to remove TruSeq adaptor sequences and bases with quality scores below 20, and reads with less than 30 remaining bases were discarded. Trimmed reads were then aligned to mm10 mouse genome with the STAR spliced-read aligner[38]. For each gene from the RefSeq annotations, the number of uniquely mapped reads overlapping with the exons was counted with HTSeq (http://www-huber.embl.de/users/anders/HTSeq/). Genes

with fewer than 50 read counts were considered as not expressed and filtered out. Principal component analysis (PCA) was performed (n = 11962) for clustering gene expression. Differential gene expression was estimated using DESeq package[39]. To determine activation related transcriptional signatures in Treg cells, the differences between read counts of peripheral activated versus resting Treg cells from wild type *Foxp3*^{gfp} mice were evaluated by fold-change and Benjamini-Hochberg corrected *P* values (FDR < 0.001) (Supplementary Data 1 and Supplementary Data 2). For gene expression comparisons, previously published transcriptional signatures of TCR dependent genes in Treg cells were used[7]. The distribution of gene expression changes is shown for transcriptional signature genes and the rest of all expressed genes. One-tailed Kolmogorov-Smirnov test is used to determine the significance between the distributions of signature genes and the rest of expressed genes.

Chromatin Immunoprecipitation

1×10^6 cells were cross-linked with 1% formaldehyde for 5 min at room temperature. Cross-linked cells were lysed and nuclei were resuspended in 250 μl nuclear lysis buffer containing 1% SDS. Chromatin input samples were prepared by sonication of cross-linked nuclear lysates. For histone ChIPs, nuclear lysates were subjected to micrococcal nuclease digestion prior to sonication. Nuclei were resuspended in 100ul MNase (New England Biolabs) at 12,000 units/ml for 1 minute at 37°C. The reaction was stopped by addition of 10 μl 0.5M EDTA. Chromatin input samples were incubated overnight at 4°C with antibodies against H3K4me1 (Abcam), H3K4me3 (Millipore), or H3K27Ac (Abcam) and precipitated for 90 minutes at 4°C using protein A Dynabeads (Life Technologies). After thorough washing, bead-bound chromatin was subjected to proteinase K digestion and decrosslinking overnight at 65°C. DNA fragments were isolated using Qiagen PCR purification kit. Relative abundance of precipitated DNA fragments was analyzed by qPCR using Power SYBR Green PCR Master Mix (Applied Biosystems). Primers used for qPCR are the followings:

Gm5069: F: TAAGCAATTGGTGGTGCAGGATGC,R: AAAGGGTCATCATCTCCGTCCGTT

Hspa2: F: TCGTGGAGAGTTGTGAGAAGCGA, R: AACGTTAGGACGAAAGCGTCAGGA

Rpl30: F: TCGGCTTCACTCACCGTCTTCTTT, R: TGTCCTCTGTGTATGCTAGGTTGG

Foxp3 Promoter:F: TAATGTGGCAGTTTCCCACAAGCC, R: AATACCTCTCTGCCACTTTCGCCA

CNS1: F: AGACTGTCTGGAACAACCTAGCCT, R: TGGAGGTACAGAGAGGTTAAGAGCCT

CNS2: F: ATCTGGCCAAGTTCAGGTTGTGAC, R: GGGCGTTCCTGTTTGACTGTTTCT

CNS3: F: TCTCCAGGCTTCAGAGATTCAAGG, R: ACAGTGGGATGAGGATACATGGCT

Relative enrichment was calculated by normalizing to background binding to the control region (*GM5069*).

Immunoglobulin isotype ELISA and immunofluorescence staining

Quantification of serum Ig isotypes was performed by ELISA as previously described[40]. Tissue sections from gender matched *Rag1*$^{-/-}$ mice were used to detect mouse autoantibodies. Briefly, organs from the *Rag1*$^{-/-}$ mice were dissected, fixed with neutral buffered formalin, embedded with paraffin and sectioned. After deparaffinization with EZPrep buffer (Ventana Medical Systems) and antigen retrieval with Cell Conditioning Solution (CC1) (Ventana Medical Systems) the sections were blocked for 30 minutes with Background Buster solution (Innovex), followed by Avidin/Biotin blocking for 8 minutes, mouse serum (1:50 dilution) incubation for 5 hours and biotinylated horse anti-mouse IgG (Vector Labs) incubation for 1 hour. The detection was performed with Streptavidin-HRP (Ventana Medical Systems) followed by incubation with Tyramide Alexa Fluor 488 (Invitrogen). The slides were then counterstained with DAPI (Sigma Aldrich) for 10 minutes, mounted, scanned with a Mirax scanner and visualized with Pannoramic Viewer (3DHISTECH). Scanned images were scored and representative snapshots were processed with Photoshop (Adobe) to switch the green and red channels for presentation purpose.

Generation of mixed bone marrow chimeras

Mixed bone marrow chimeras were generated as previously described[31]. Briefly, recipient mice were irradiated (9.5 Gy) 24h before i.v. injection of 10×10^6 bone marrow cells from CD45.1 *Foxp3*^{gfp} and CD45.2 *Foxp3*$^{\Delta CNS3\text{-}gfp}$ mixed at a 1:1 ratio. After bone marrow transfer, the recipient mice were administrated with 2mg/ml neomycin in drinking water for 3 weeks and analyzed 8-10 weeks later.

Histological Analysis

Tissue samples were fixed in 10% neutral buffered formalin and processed for hematoxylin and eosin staining. Stained slides were scored for tissue inflammation as previously described[41].

EAE induction

EAE was induced by immunization with myelin oligodendrocyte glycoprotein peptide 35-55 (MOG35-55, GenScript) in Complete Freund's Adjuvant (CFA, Sigma) and mice were monitored for disease as previously described[42].

Extended Data

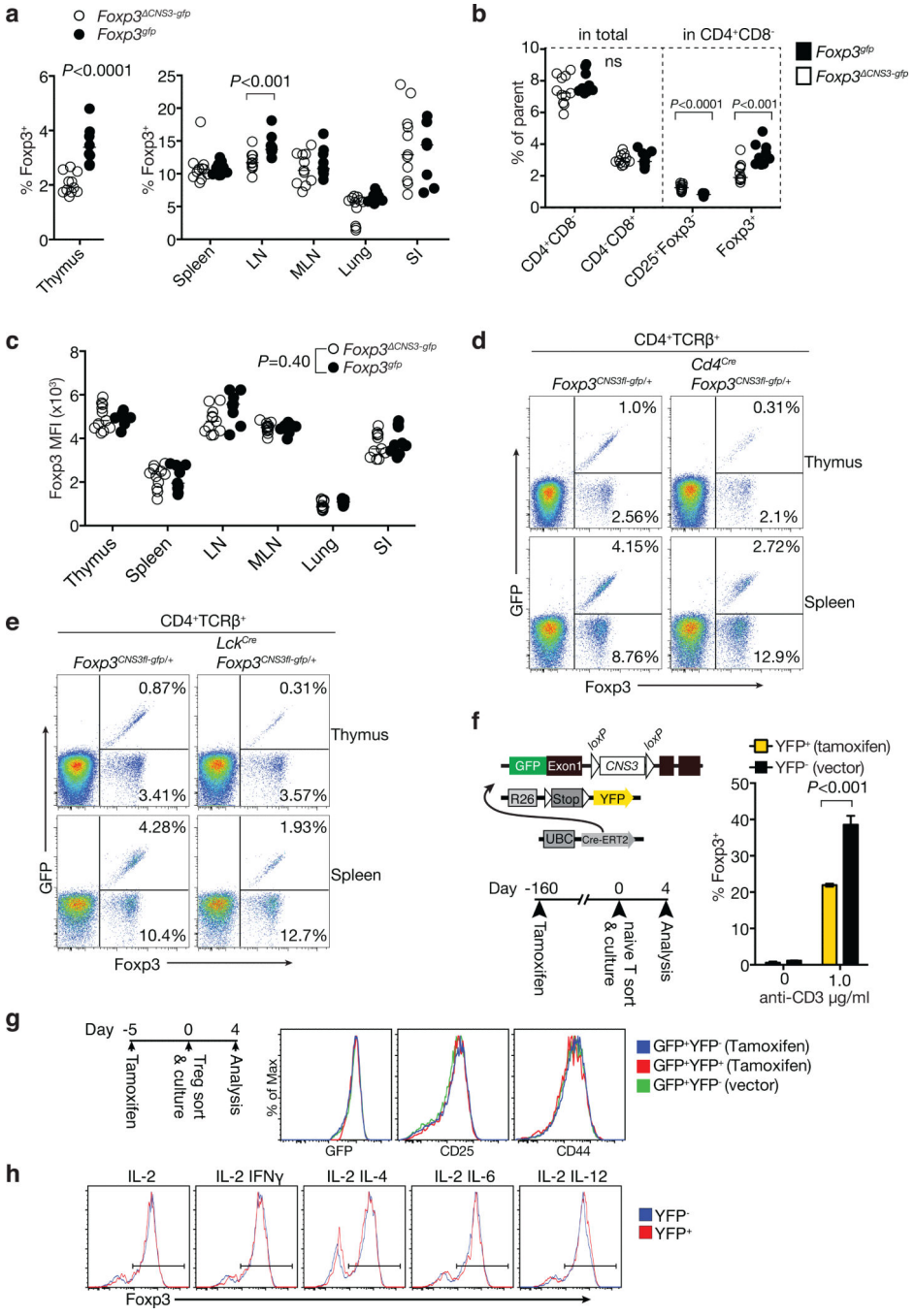

Extended Data Figure 1. *CNS3* is required in precursor cells for optimal Treg cell differentiation

a, Diminished numbers of thymic Treg cells in 6-8 week old *CNS3*-deficient mice. Two-tailed Mann Whitney test. The data show individual mice and median, and represent one of >2 independent experiments. $Foxp3^{gfp}$ (n=9) $Foxp3^{\Delta CNS3\text{-}gfp}$ (n=11). LN, lymph nodes. MLN, mesenteric lymph nodes. SI, small intestine.

b, c, Flow cytometric analysis of CD4 and CD8 single positive thymocyte subsets including thymic Treg precursor ($CD25^+Foxp3^-$ $CD4^+$) cells (**b**) and Foxp3 expression (**c**) in 6-8 week old $Foxp3^{\Delta CNS3\text{-}gfp}$ mice (n=11) and $Foxp3^{gfp}$ (n=9) littermates. Unpaired Mann Whitney test was used for statistical analysis.

d, e, *CNS3*-dependent Treg cell differentiation in heterozygous $Foxp3^{CNS3fl\text{-}gfp/+}$ and $Cd4^{Cre}$ $Foxp3^{CNS3fl\text{-}gfp/+}$ (**d**), or $Foxp3^{CNS3fl\text{-}gfp/+}$ and Lck^{Cre} $Foxp3^{CNS3fl\text{-}gfp/+}$ females (**e**). GFP^+ and GFP^- Treg cells in these mice express $Foxp3^{CNS3fl\text{-}gfp}$ or wild-type $Foxp3^+$ alleles, respectively. The data represent one of >2 independent experiments (≥ 3 mice per group).

f, Acute ablation of *CNS3* impairs Treg induction *in vitro*. YFP^+ (tamoxifen treated) or YFP^- (vector control) naïve $CD4^+$ T cells from $UBC^{Cre\text{-}ERT2}$ $Foxp3^{CNS3fl\text{-}gfp}$ R26Y males were cultured under *in vitro* Treg induction conditions. The data show mean ± SEMs of triplicate cultures and represent one of two independent experiments. Two-tailed unpaired t-test.

g, h, Acute ablation of *CNS3* in differentiated Treg cells does not affect Foxp3 expression level on a per cell basis or the stability of mature Treg cells. Expression of Foxp3, CD25 and CD44 in Treg cells on day 4 after tamoxifen treatment (**g**). YFP^+ and YFP^- Treg cells from tamoxifen treated $UBC^{Cre\text{-}ERT2}$ $Foxp3^{CNS3fl\text{-}gfp}$ R26Y males were cultured in the presence of IL-2, IFNγ, IL-4, IL-6, and IL-12 for 4 days (**h**). The data represent two independent experiments.

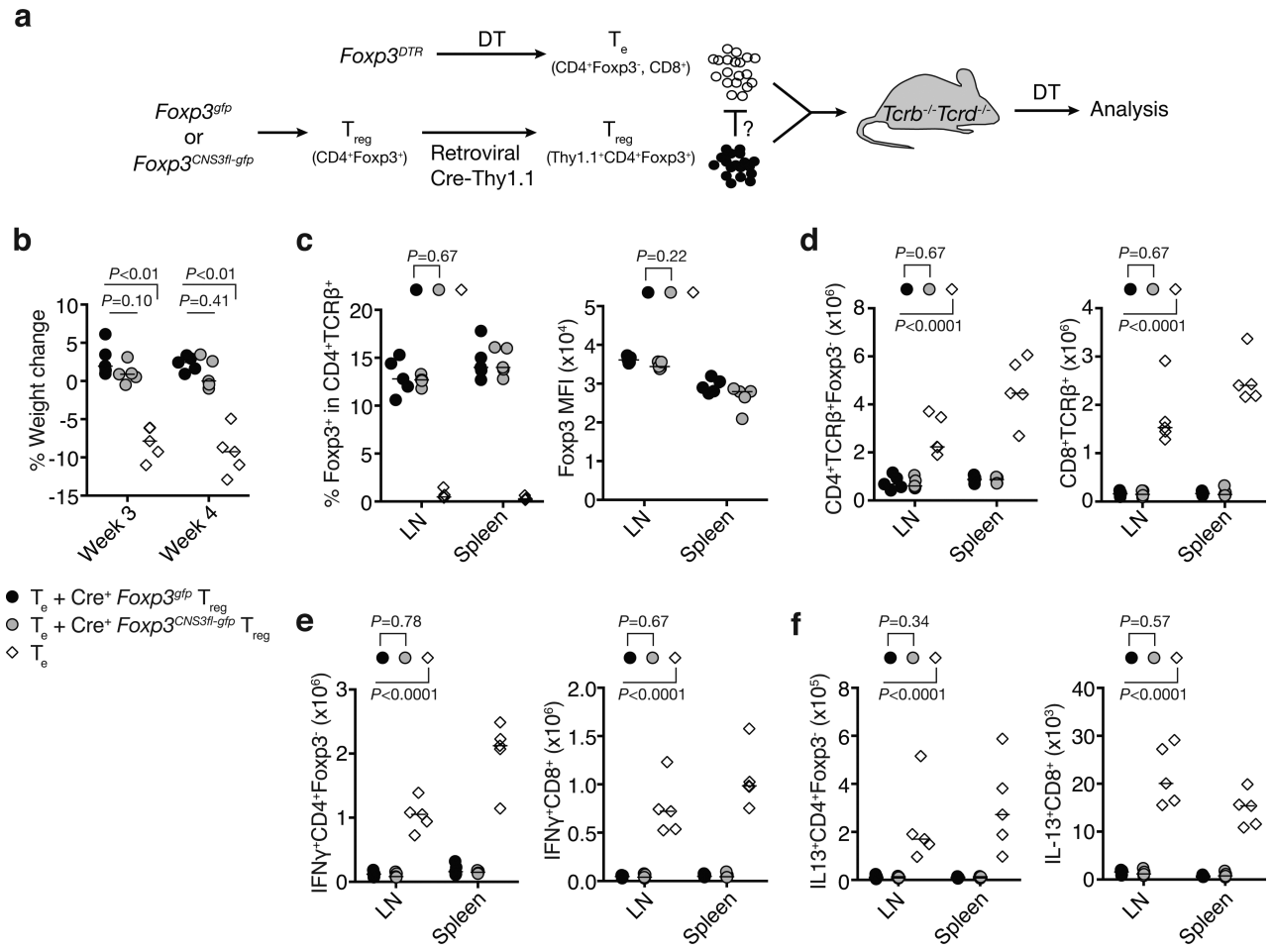

Extended Data Figure 2. *CNS3* is dispensable for the suppressor function of differentiated Treg cells *in vivo*

In vivo assessment of the suppressor function of Treg cells upon acute ablation of *CNS3*. Treg cells ($CD4^+GFP^+$) isolated from *Foxp3*^{gfp} or *Foxp3*$^{CNS3fl\text{-}gfp}$ mice were activated with CD3 and CD28 antibody coated beads *in vitro* for five days and then transduced with retroviruses expressing Cre recombinase and a Thy1.1 reporter. Three days later, $Thy1.1^+CD4^+GFP^+$ cells were sorted by FACS for the suppressor assay. $CD4^+Foxp3^-$ and $CD8^+$ effector T cells (Te) sorted from *Foxp3*^{DTR} reporter mice seven days after diphtheria toxin (DT) injection (1μg i.p. per mouse) were transferred alone or with equal amounts of $Thy1.1^+$ Cre transduced *Foxp3*^{gfp} or *Foxp3*$^{CNS3fl\text{-}gfp}$ Treg cells into *Tcrb*$^{-/-}$*Tcrd*$^{-/-}$ recipients (**a**). Mice were weighted before and after T cell transfer, and relative weight changes were assessed at week 3 and week 4 post transfer (**b**). Four weeks after adoptive transfer, cells were recovered and analyzed for Treg frequencies and Foxp3 expression (**c**), $CD4^+TCR\beta^+Foxp3^-$ and $CD8^+TCR\beta^+$ cell numbers (**d**), IFNγ (**e**) and IL-13 (**f**) production. Unpaired Mann Whitney test was used for statistical analysis (n=5 per group).

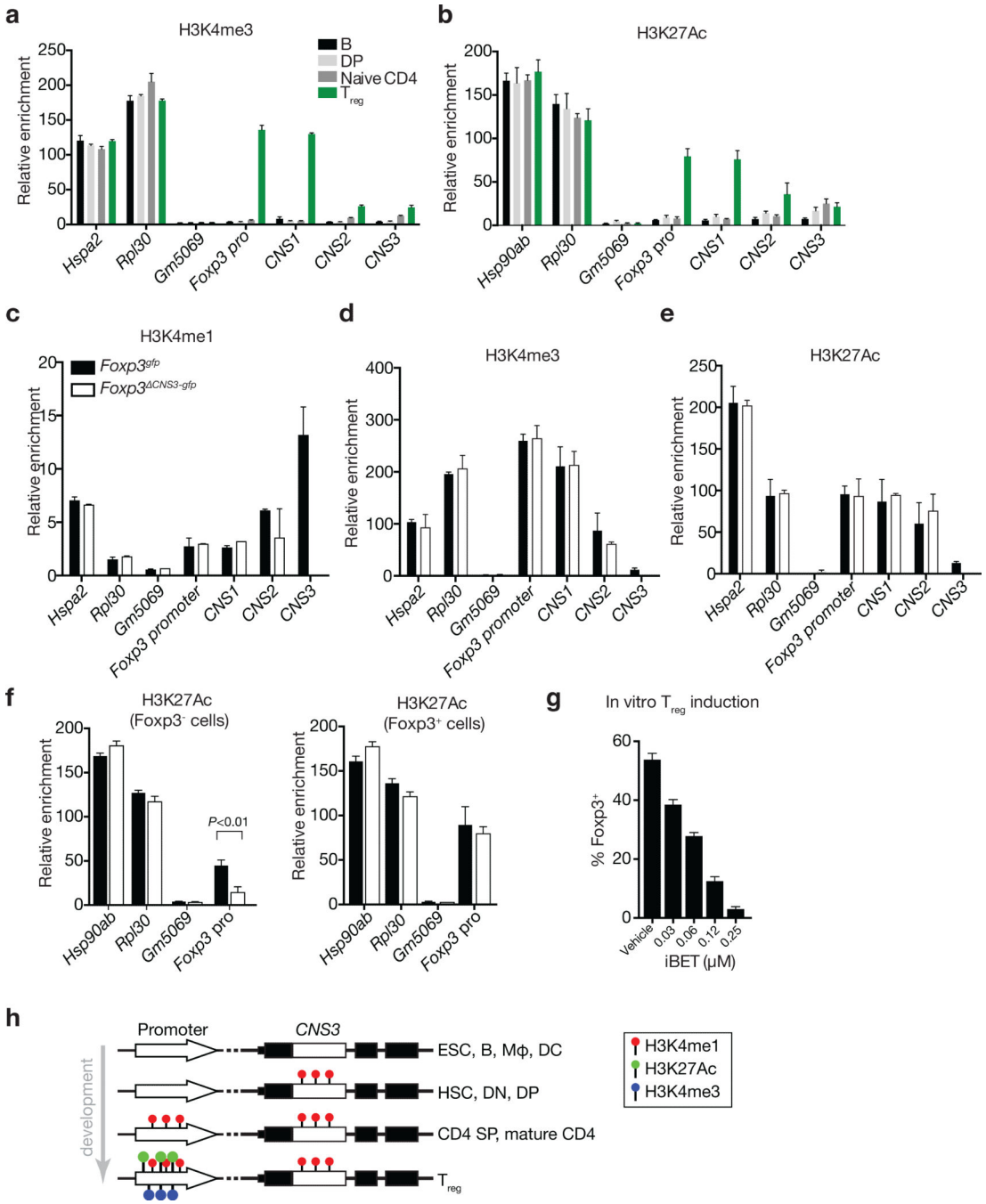

Extended Data Figure 3. Epigenetic modifications at the *Foxp3* locus during Treg differentiation

a, b, ChIP-qPCR analysis of H3K4me3 (**a**) and H3K27Ac (**b**) at the *Foxp3* locus and control loci (*Hspa2*, *Rpl30* and *Gm5069*) in B cells, DP thymocytes, naïve CD4$^+$ T and Treg cells. FACS sorted cells from wild type male *Foxp3^{DTR}* mice were used for ChIP-qPCR. Relative enrichment was calculated by normalizing to background binding to control region (*GM5069*).

c-e, ChIP-qPCR analysis of H3K4me1 (**c**), H3K4me3 (**d**) and H3K27Ac (**e**) in the *Foxp3* locus in mature Treg cells isolated from wild type $Foxp3^{gfp}$ and $Foxp3^{\Delta CNS3\text{-}gfp}$ male mice normalized to the background binding to the *Gm5069* locus.

f, *CNS3*-dependent deposition of H3K27Ac at the *Foxp3* promoter in Foxp3$^-$ CD4$^+$ T cells during *in vitro* Treg cell induction. $Foxp3^{gfp}$ or $Foxp3^{\Delta CNS3\text{-}gfp}$ naïve CD4$^+$ T cells were cultured under *in vitro* Treg cell differentiation conditions. After three days of culture, GFP$^-$ and GFP$^+$ cells were sorted for ChIP-qPCR analysis. Two-tailed unpaired t-test.

g, Inhibition of Treg induction *in vitro* by bromodomain protein inhibitor iBET. Naïve CD4$^+$ T cells from wild type $Foxp3^{gfp}$ males were used for Foxp3 *in vitro* induction in the presence of indicated concentrations of iBET or vehicle.

h, Schematic of the chromatin dynamics at *CNS3* and the *Foxp3* promoter during Treg cell differentiation.

The data are shown as means ± SEMs of triplicates and represent one of two independent experiments.

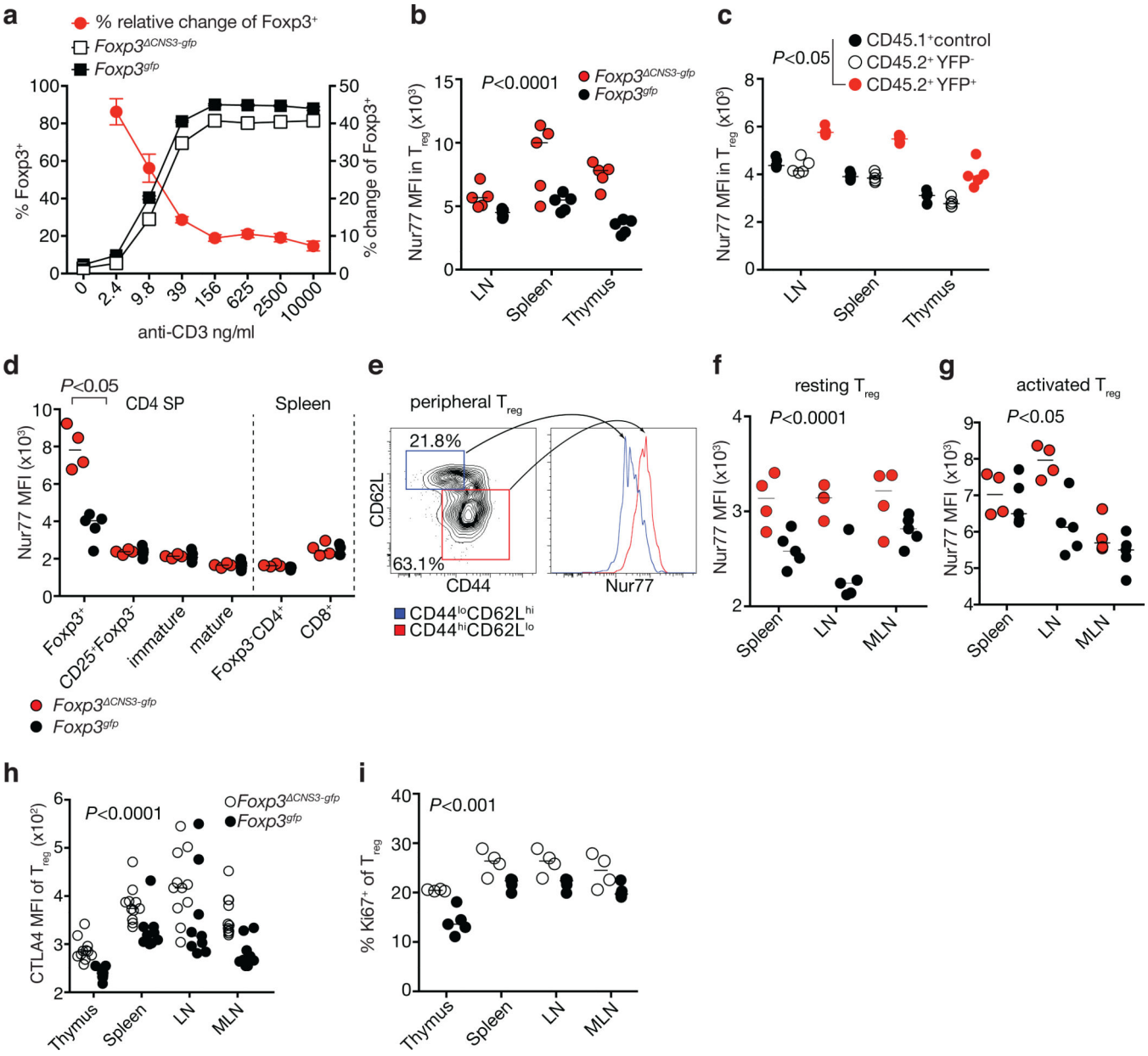

Extended Data Figure 4. *CNS3* facilitates Foxp3 induction and shapes Treg cell repertoire

a, Differential impact of *CNS3* on Treg cell *in vitro* development of mature non-Treg CD4 single positive T cells. CD4 single positive thymocytes ($CD4^+CD8^-TCR\beta^{hi}GFP^-CD25^-CD69^{lo}CD62L^{hi}$) were pooled and sorted from male *Foxp3*^{gfp} and *Foxp3*$^{\Delta CNS3\text{-}gfp}$ littermates (n=7 each group) for *in vitro* Treg induction performed with titrated CD3 antibody and lethally irradiated antigen presenting cells isolated from wild type B6 spleens in the presence of TGFβ and recombinant IL-2. Foxp3 expression was analyzed four days later and the relative changes of the ratios of Foxp3 expressing cells in the absence of *CNS3* was calculated by comparing to *CNS3*-sufficient groups. Data depict means ± SEMs of five replicate cultures and represent one of three independent experiments.

b, Flow cytometric analysis of Nur77 protein expression in *CNS3*-deficient and -sufficient Treg cells. (n=5 each group). Two-tailed unpaired Mann Whitney test. The data represent one of >2 independent experiments.

c, Elevated Nur77 protein levels in *CNS3*-deficient Treg cells developed after conditional ablation of *CNS3* upon tamoxifen induced activation of $UBC^{Cre\text{-}ERT2}$. Bone marrow of CD45.1 $Foxp3^{gfp}$ and CD45.2 $UBC^{Cre\text{-}ERT2}$ $Foxp3^{CNS3fl\text{-}gfp}$ R26Y mice were collected from donor mice treated with tamoxifen, mixed at a 1:1 ratio and transferred into lethally irradiated $Tcrb^{-/-}Tcrd^{-/-}$ recipients. $CD45.1^{+}CD4^{+}GFP^{+}$, $CD45.2^{+}YFP^{-}GFP^{+}$ and $CD45.2^{+}YFP^{+}GFP^{+}$ cells were sorted for flow cytometric analysis of Nur77 protein levels 10 weeks after BM transfer (n=5). Unpaired Mann Whitney tests were used to compare $CD45.2^{+}YFP^{+}GFP^{+}$ and $CD45.2^{+}YFP^{-}GFP^{+}$ or $CD45.2^{+}YFP^{+}GFP^{+}$ and control ($CD45.1^{+}CD4^{+}GFP^{+}$) groups. The data show medians of individual mice and represent more than three independent experiments.

d, Nur77 expression levels in thymic Treg precursors ($CD25^{+}Foxp3^{-}$), immature ($CD69^{hi}CD62L^{lo}$) and mature ($CD69^{lo}CD62L^{hi}$) CD4 SP thymocytes, and peripheral $Foxp3^{-}CD4^{+}$ and $CD8^{+}$ T cells in 6-7 week old $Foxp3^{gfp}$ (n=5) and $Foxp3^{\Delta CNS3\text{-}gfp}$ (n=4) littermates. Unpaired Mann Whitney test was used for statistical analysis. The data show medians of individual mice and represent more than three independent experiments.

e, Differential Nur77 expression in peripheral resting ($CD62L^{hi}CD44^{lo}$) and activated ($CD62L^{lo}CD44^{hi}$) Treg cells (wild type $Foxp3^{gfp}$). The data represent one of more than three independent experiments.

f, g, Upregulation of Nur77 expression in resting ($CD62L^{hi}CD44^{lo}$) (**f**) and activated ($CD44^{hi}CD62L^{lo}$) (**g**) *CNS3*-deficient Treg cells in 6-7 week old $Foxp3^{gfp}$ (n=5) and $Foxp3^{\Delta CNS3\text{-}gfp}$ (n=4) littermates. Unpaired Mann Whitney test; the data represent at least three experiments.

h, i, CTLA4 (**h**) and Ki67 (**i**) expression by *CNS3*-deficient and -sufficient Treg cells in $Foxp3^{gfp}$ (n=9) and $Foxp3^{\Delta CNS3\text{-}gfp}$ (n=11) mice (**h**). n=5 $Foxp3^{gfp}$, n=4 $Foxp3^{\Delta CNS3\text{-}gfp}$ (**i**). Two-tailed unpaired Mann Whitney test. The data represent one of >3 independent experiments.

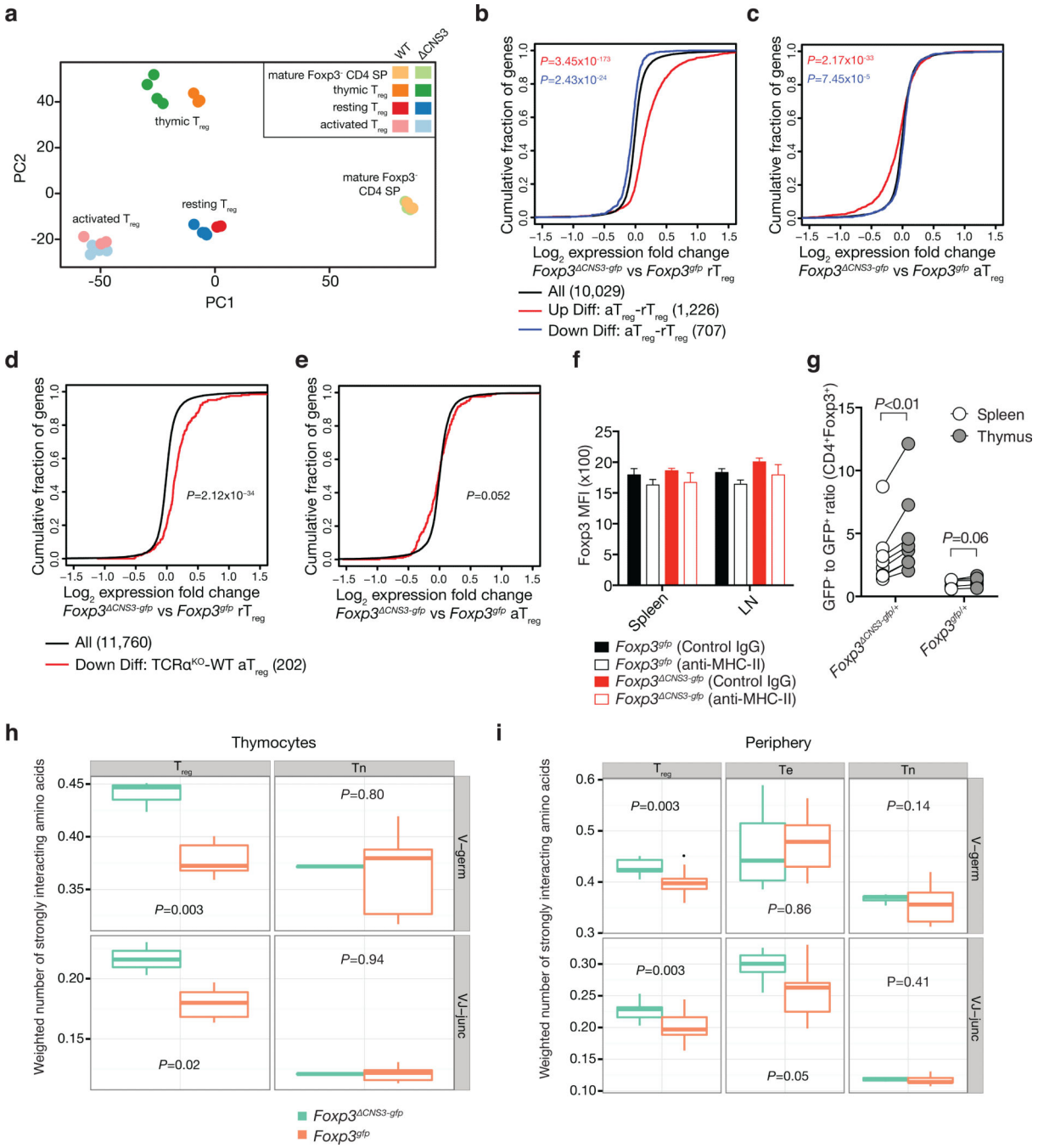

Extended Data Figure 5. Influence of *CNS3* on Treg cell repertoire

a, Principal component analysis of mRNA expression in *CNS3*-deficient and -sufficient mature Foxp3^{-} and Foxp3^{+} CD4 SP thymocytes, and peripheral resting and activated Treg cells. RNA-seq was performed with three and four biological replicates for cells sorted from male *Foxp3^{gfp}* and *Foxp3$^{\Delta CNS3\text{-}gfp}$* littermates, respectively. Dots represent samples from individual mice.

b, c, Relative gene expression levels (cumulative fraction of genes) in *CNS3*-sufficient and -deficient peripheral resting Treg cells (rTreg) (**b**) or activated Treg cells (aTreg) (**c**) in

comparison to those up- and down-regulated in activated versus resting Treg cells isolated from *Foxp3*^{gfp} mice. The numbers of genes in each comparison group are indicated in parentheses.

d, e, Relative gene expression levels in *CNS3*-sufficient and -deficient peripheral rTreg (**d**) or aTreg cells (**e**) in comparison to those down-regulated in activated Treg cells subjected to acute TCR ablation versus mock treatment. The numbers of genes in each comparison group are indicated in parentheses.. Statistical analysis was performed using one-tailed Kolmogorov-Smirnov test.

f, Flow cytometric analysis of Foxp3 expression level (MFI) in *CNS3*-sufficient and deficient Treg cells after expansion in lymphopenic recipients. Treg cells were sorted from mixed bone marrow chimeras of CD45.1 *Foxp3*^{gfp} and CD45.2 *Foxp3*$^{\Delta CNS3\text{-}gfp}$ mice and mixed at a 1:1 ratio, and co-transferred with wild type naïve Foxp3^{-}CD4^{+} T cells into *Tcrb*$^{-/-}$*Tcrd*$^{-/-}$ recipients treated with MHC class II blocking antibody or isotype control IgG before and after the transfer (n=5 per group). Means ± SEMs. The data represent one of three independent experiments. Unpaired t-test revealed no statistically significant difference between matched *CNS3*-deficient and -sufficient groups (P>0.3).

g, Comparison of *CNS3*-sufficient and -deficient Treg cells in competitive environment of heterozygous *Foxp3*$^{gfp/+}$ and *Foxp3*$^{\Delta CNS3\text{-}gfp/+}$ females (6-8 week of age). In contrast to *CNS3*-sufficient Treg cells, *CNS3*-deficient ones are relatively enriched in the periphery in comparison with those in thymus. Ratios of GFP^{-} to GFP^{+} Treg cells are inversely proportional to the relative abundance of *Foxp3*^{gfp} or *Foxp3*$^{\Delta CNS3\text{-}gfp}$ Treg cells in the Treg pool. Wilcoxon matched-pairs signed rank test, n=5 *Foxp3*$^{gfp/+}$ and n=8 *Foxp3*$^{\Delta CNS3\text{-}gfp/+}$. Linked circles represent samples from the same mice. Data represent one of two independent experiments.

h, i, Numbers of strongly interacting amino acid residues (LFIMVWCY) were calculated for the V-segment part of TCRα CDR3 (binned to germline) and V-J segment junction, and weighted by the corresponding clonotype frequencies. Sums of the weighted scores were used for the comparisons between *CNS3*-deficient and -sufficient groups (unpaired t-test). The data represent the analysis of pooled TCR sequences derived from the indicated thymic (**h)** and peripheral (**i**) CD4^{+} naïve (Tn), activated effector (Te) and Treg cell subsets isolated from individual *Foxp3*^{gfp} (n=5) and *Foxp3*$^{\Delta CNS3\text{-}gfp}$ mice (n=3). Box-and-whisker plots show minimum, maximum, first and third quartiles and median.

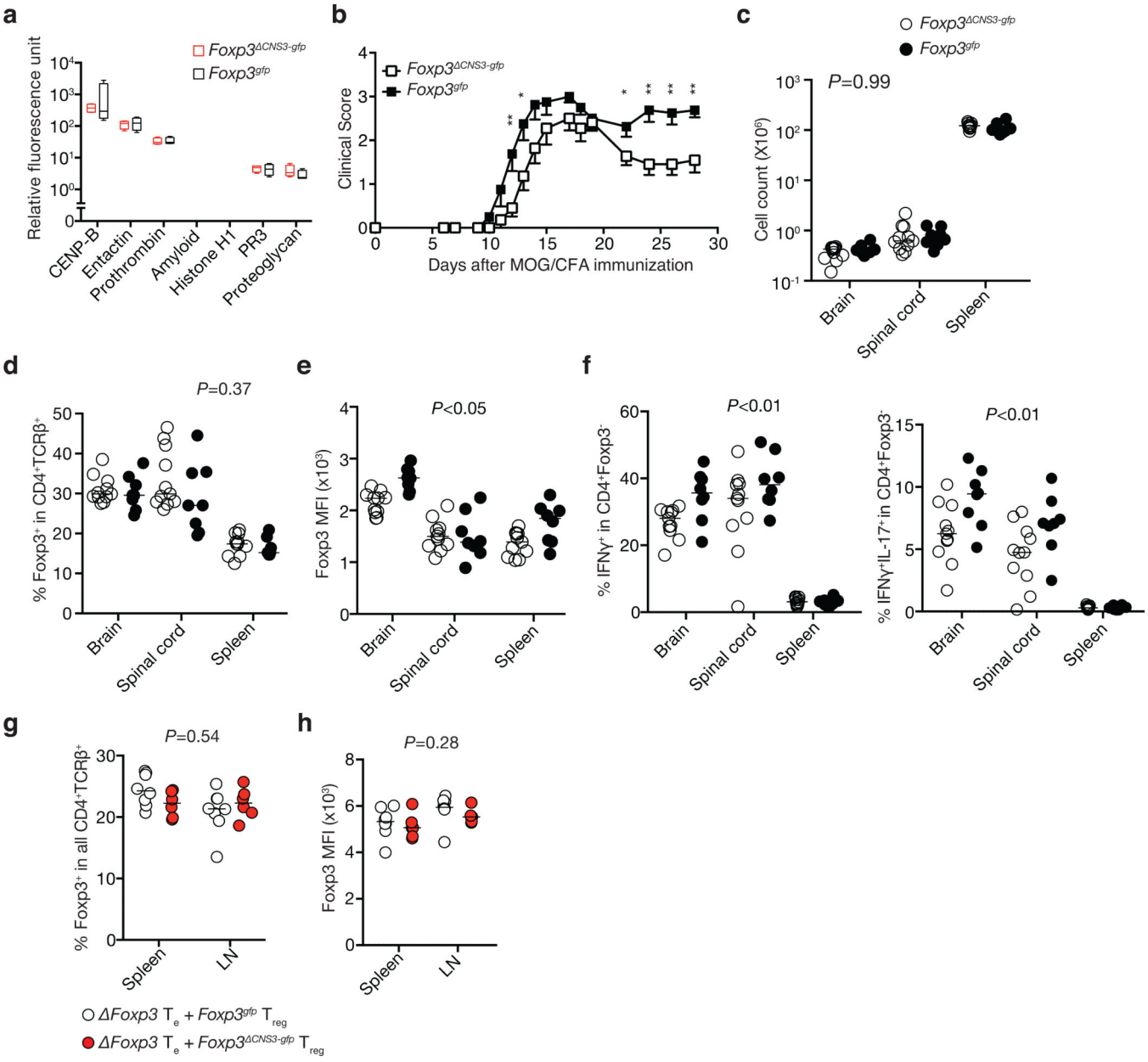

Extended Data Figure 6. Selective modulation of autoimmune responses in mice lacking *CNS3*

a, *CNS3* deficiency does not affect antibody production against a subset of autoantigens. *Foxp3*$^{\Delta CNS3\text{-}gfp}$ and *Foxp3*^{gfp} littermates (n=4 per group). Box-and-whisker plots show minimum, maximum, first and third quartiles and median. Data represent one of two independent experiments.

b-f, *CNS3* deficiency decreases EAE severity. Upon immunization with MOG peptide in CFA mice of indicated genotypes were assessed for the severity of limb paralysis (**b**), effector T cell numbers (**c**), Treg frequency (**d**), Foxp3 expression level (**e**) and inflammatory cytokine production (**f**). *Foxp3*^{gfp} (n=8), *Foxp3*$^{\Delta CNS3\text{-}gfp}$ (n=11). Unpaired t-test (**b**) or Mann Whitney test (**c-f**) were used to compare *Foxp3*^{gfp} and *Foxp3*$^{\Delta CNS3\text{-}gfp}$ groups. Means -SEMs (**b**). * $P<0.05$, ** $P<0.01$. The data represent 2 independent experiments.

g-h, Analysis of the proportion of Treg cells in $CD4^{+}TCR\beta^{+}$ cell population (**g**) and level of Foxp3 expression (MFI) (**h**) in *in vivo* suppressor assay of *CNS3*-deficient or -sufficient Treg cells (Fig. 3e-h). Two-tailed unpaired Mann Whitney test.

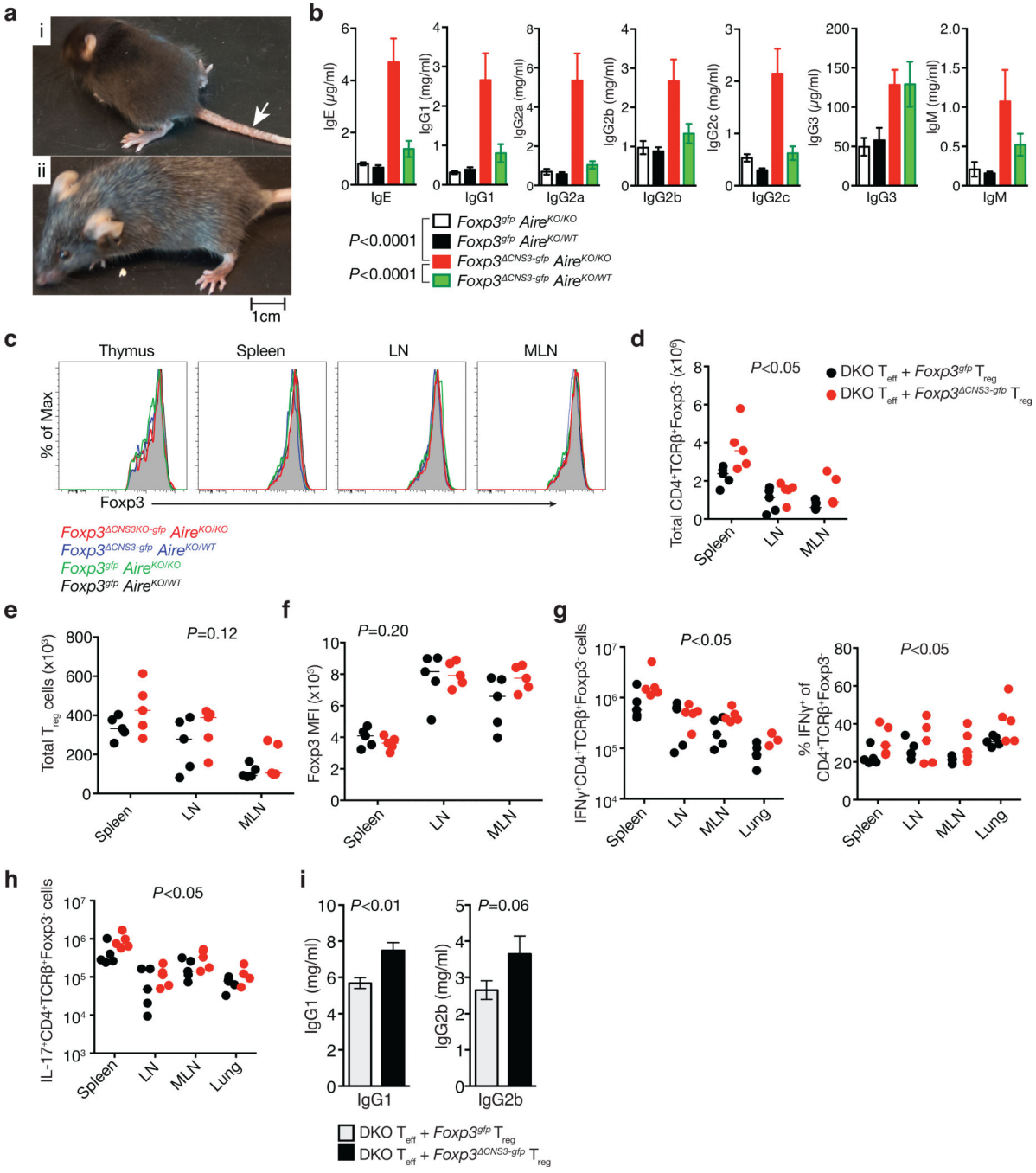

Extended Data Figure 7. Compromised suppressive function of *CNS3*-deficient Treg cells

a, Autoimmune diseases in *Foxp3*$^{\Delta CNS3\text{-}gfp}$ *Aire*$^{KO/KO}$ (DKO) mice. Arrow indicates the inflammatory lesions in the tail of a three week-old mouse with an early onset of

autoimmunity (n>11) (i). Depigmentation in a six week-old mouse with delayed onset of autoimmunity (n>16) (ii).

b, Analysis of serum Ig isotypes in *Foxp3*$^{\Delta CNS3\text{-}gfp}$ *Aire*$^{KO/KO}$ and littermate control mice using ELISA (n=8 each group). Mean ± SEMs. The statistical analysis was performed using a two-way ANOVA. **c**, Flow cytometric analysis of Foxp3 expression by Treg cells. The data show one of at least three mice per group and represent more than three independent experiments.

d-i, Analysis of the ability of *CNS3*-deficient and -sufficient Treg cells to control *CNS3 Aire* DKO effector T cells upon adoptive transfer into T cell deficient recipients. Flow cytometric analysis of non-Treg CD4$^+$ T cell numbers (**d**), Treg cell numbers (**e**), Foxp3 expression level (**f**), and IFNγ production (**g**), IL-17 production (**h**), and serum IgG1 and IgG2b levels (**i**) in recipient mice transferred with *CNS3 Aire* DKO effector T cells (Foxp3$^-$CD4$^+$ and CD8$^+$) at a 10:1 ratio with Treg cells from *Aire*-sufficient *Foxp3*^{gfp} or *Foxp3*$^{\Delta CNS3\text{-}gfp}$ mice. *P* values show the comparisons between the two groups performed using two-tailed unpaired Mann Whitney tests (**d-h**) or unpaired t-test (**i**). Mean ± SEMs (**i**). The recipient mice were analyzed 7 weeks after adoptive T cell transfer (n=5 per group).

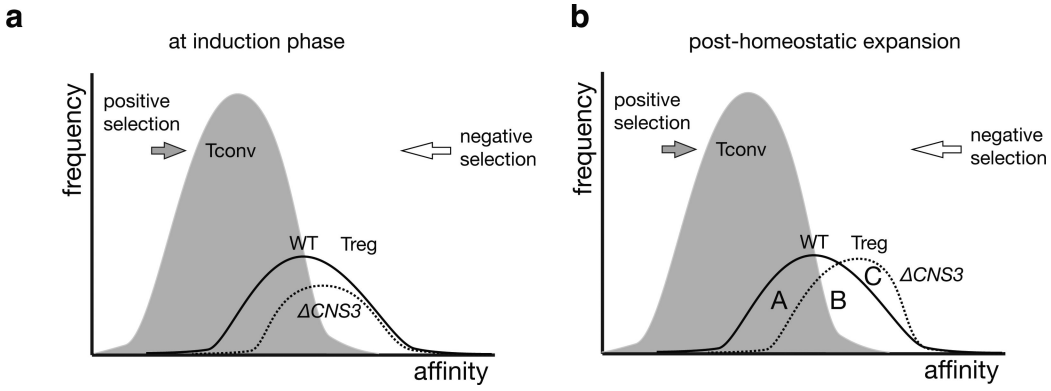

Extended Data Figure 8. Theoretical impact of *CNS3* on Treg TCR repertoire

a, Hypothetical distribution of TCRs expressed by Treg and non-Treg CD4$^+$ T cells according to their affinities for self-antigens. Precursor cells expressing TCRs within a certain low affinity window are positively selected and become “conventional” CD4$^+$ T cells, and those with higher affinities for self-antigens differentiate into Treg cells. *CNS3* promotes the differentiation of Treg cells and broadens their TCR repertoire by facilitating Foxp3 expression predominantly in response to lower strength (“suboptimal”) of inducing TCR signals.

b, Upon expansion in the periphery, *CNS3*-deficient Treg cells reach similar numbers as their wild type counterparts, with some TCRs underrepresented (A), some minimally affected (B), and some overrepresented (C). T_{CONV}: conventional T cells.

Supplementary Material

Refer to Web version on PubMed Central for supplementary material.

ACKNOWLEDGEMENTS

We thank P. Bos, A. Arvey, C. Konopacki, G. Gasteiger, S. Lee, T. Chinen, and K. Wu for technical assistance, R. Prinjha for providing iBET. Y.F. was supported by a Postdoctoral Fellowship of the Cancer Research Institute. This study was supported by NIH grant R37 AI034206 and U01 HG007893, Cancer Center Support Grant P30 CA008748, and the Howard Hughes Medical Institute (A.Y.R.). M.S., E.V.P., and D.M.C. were supported by MCB program RAS and RFBR grants 14-04-01247 and 15-34-21052.

REFERENCES

1. Klein L, Kyewski B, Allen PM, Hogquist KA. Positive and negative selection of the T cell repertoire: what thymocytes see (and don't see). Nat Rev Immunol. 2014; 14:377–391. doi:10.1038/nri3667. [PubMed: 24830344]
2. Josefowicz SZ, Lu LF, Rudensky AY. Regulatory T cells: mechanisms of differentiation and function. Annu Rev Immunol. 2012; 30:531–564. doi:10.1146/annurev.immunol.25.022106.141623. [PubMed: 22224781]
3. Chandra, S.; Kronenberg, M. Advances in immunology. Academic Press; 2015.
4. Hsieh CS, Zheng Y, Liang Y, Fontenot JD, Rudensky AY. An intersection between the self-reactive regulatory and nonregulatory T cell receptor repertoires. Nat Immunol. 2006; 7:401–410. doi:ni1318 [pii] 10.1038/ni1318. [PubMed: 16532000]
5. Hsieh CS, et al. Recognition of the peripheral self by naturally arising CD25+ CD4+ T cell receptors. Immunity. 2004; 21:267–277. doi:10.1016/j.immuni.2004.07.009 S1074761304001979 [pii]. [PubMed: 15308106]
6. Lee HM, Bautista JL, Scott-Browne J, Mohan JF, Hsieh CS. A broad range of self-reactivity drives thymic regulatory T cell selection to limit responses to self. Immunity. 2012; 37:475–486. doi:10.1016/j.immuni.2012.07.009. [PubMed: 22921379]
7. Levine AG, Arvey A, Jin W, Rudensky AY. Continuous requirement for the TCR in regulatory T cell function. Nat Immunol. 2014; 15:1070–1078. doi:10.1038/ni.3004. [PubMed: 25263123]
8. Jordan MS, et al. Thymic selection of CD4+CD25+ regulatory T cells induced by an agonist self-peptide. Nat Immunol. 2001; 2:301–306. doi:10.1038/86302. [PubMed: 11276200]
9. Lafaille JJ, Nagashima K, Katsuki M, Tonegawa S. High incidence of spontaneous autoimmune encephalomyelitis in immunodeficient anti-myelin basic protein T cell receptor transgenic mice. Cell. 1994; 78:399–408. [PubMed: 7520367]
10. Apostolou I, Sarukhan A, Klein L, von Boehmer H. Origin of regulatory T cells with known specificity for antigen. Nat Immunol. 2002; 3:756–763. doi:10.1038/ni816. [PubMed: 12089509]
11. Zheng Y, et al. Role of conserved non-coding DNA elements in the Foxp3 gene in regulatory T-cell fate. Nature. 2010; 463:808–812. doi:nature08750 [pii] 10.1038/nature08750. [PubMed: 20072126]
12. Fontenot JD, et al. Regulatory T cell lineage specification by the forkhead transcription factor foxp3. Immunity. 2005; 22:329–341. doi:S1074-7613(05)00066-X [pii] 10.1016/j.immuni.2005.01.016. [PubMed: 15780990]
13. Setoguchi R, Hori S, Takahashi T, Sakaguchi S. Homeostatic maintenance of natural Foxp3(+) CD25(+) CD4(+) regulatory T cells by interleukin (IL)-2 and induction of autoimmune disease by IL-2 neutralization. J Exp Med. 2005; 201:723–735. doi:10.1084/jem.20041982. [PubMed: 15753206]
14. Fontenot JD, Rasmussen JP, Gavin MA, Rudensky AY. A function for interleukin 2 in Foxp3-expressing regulatory T cells. Nat Immunol. 2005; 6:1142–1151. doi:ni1263 [pii] 10.1038/ni1263. [PubMed: 16227984]
15. Seddon B, Legname G, Tomlinson P, Zamoyska R. Long-term survival but impaired homeostatic proliferation of Naive T cells in the absence of p56lck. Science. 2000; 290:127–131. [PubMed: 11021796]
16. Nicodeme E, et al. Suppression of inflammation by a synthetic histone mimic. Nature. 2010; 468:1119–1123. doi:10.1038/nature09589. [PubMed: 21068722]

17. Arpaia N, et al. Metabolites produced by commensal bacteria promote peripheral regulatory T-cell generation. Nature. 2013 doi:10.1038/nature12726.
18. Davie JR. Inhibition of histone deacetylase activity by butyrate. The Journal of nutrition. 2003; 133:2485S–2493S. [PubMed: 12840228]
19. Furusawa Y, et al. Commensal microbe-derived butyrate induces the differentiation of colonic regulatory T cells. Nature. 2013 doi:10.1038/nature12721.
20. Moran AE, et al. T cell receptor signal strength in Treg and iNKT cell development demonstrated by a novel fluorescent reporter mouse. J Exp Med. 2011 doi:jem.20110308 [pii] 10.1084/jem.20110308.
21. Zikherman J, Parameswaran R, Weiss A. Endogenous antigen tunes the responsiveness of naive B cells but not T cells. Nature. 2012; 489:160–164. doi:10.1038/nature11311. [PubMed: 22902503]
22. Shugay M, et al. Towards error-free profiling of immune repertoires. Nat Methods. 2014; 11:653–655. doi:10.1038/nmeth.2960. [PubMed: 24793455]
23. Shugay M, et al. VDJtools: unifying post-analysis of T cell receptor repertoires. PLoS Comput Biol. In Press.
24. Kosmrlj A, Jha AK, Huseby ES, Kardar M, Chakraborty AK. How the thymus designs antigen-specific and self-tolerant T cell receptor sequences. Proc Natl Acad Sci U S A. 2008; 105:16671–16676. doi:10.1073/pnas.0808081105. [PubMed: 18946038]
25. Yang S, Fujikado N, Kolodin D, Benoist C, Mathis D. Immune tolerance. Regulatory T cells generated early in life play a distinct role in maintaining self-tolerance. Science. 2015; 348:589–594. doi:10.1126/science.aaa7017. [PubMed: 25791085]
26. Klein L, Hinterberger M, Wirnsberger G, Kyewski B. Antigen presentation in the thymus for positive selection and central tolerance induction. Nat Rev Immunol. 2009; 9:833–844. doi:nri2669 [pii] 10.1038/nri2669. [PubMed: 19935803]
27. Liston A, Lesage S, Wilson J, Peltonen L, Goodnow CC. Aire regulates negative selection of organ-specific T cells. Nat Immunol. 2003; 4:350–354. doi:10.1038/ni906. [PubMed: 12612579]
28. Giraud M, et al. Aire unleashes stalled RNA polymerase to induce ectopic gene expression in thymic epithelial cells. Proc Natl Acad Sci U S A. 2012; 109:535–540. doi:10.1073/pnas.1119351109. [PubMed: 22203960]
29. Malchow S, et al. Aire-dependent thymic development of tumor-associated regulatory T cells. Science. 2013; 339:1219–1224. doi:10.1126/science.1233913. [PubMed: 23471412]
30. Yates AJ. Theories and quantification of thymic selection. Frontiers in immunology. 2014; 5:13. doi:10.3389/fimmu.2014.00013. [PubMed: 24550908]
31. Feng Y, et al. Control of the inheritance of regulatory T cell identity by a cis element in the Foxp3 locus. Cell. 2014; 158:749–763. doi:10.1016/j.cell.2014.07.031. [PubMed: 25126783]
32. Janeway CA Jr. et al. Monoclonal antibodies specific for Ia glycoproteins raised by immunization with activated T cells: possible role of T cellbound Ia antigens as targets of immunoregulatory T cells. J Immunol. 1984; 132:662–667. [PubMed: 6228596]
33. Stefanova I, Dorfman JR, Germain RN. Self-recognition promotes the foreign antigen sensitivity of naive T lymphocytes. Nature. 2002; 420:429–434. doi:10.1038/nature01146. [PubMed: 12459785]
34. Li QZ, et al. Identification of autoantibody clusters that best predict lupus disease activity using glomerular proteome arrays. J Clin Invest. 2005; 115:3428–3439. doi:10.1172/JCI23587. [PubMed: 16322790]
35. Egorov ES, et al. Quantitative Profiling of Immune Repertoires for Minor Lymphocyte Counts Using Unique Molecular Identifiers. J Immunol. 2015 doi:10.4049/jimmunol.1500215.
36. Britanova OV, et al. Age-related decrease in TCR repertoire diversity measured with deep and normalized sequence profiling. J Immunol. 2014; 192:2689–2698. doi:10.4049/jimmunol.1302064. [PubMed: 24510963]
37. Bolger AM, Lohse M, Usadel B. Trimmomatic: a flexible trimmer for Illumina sequence data. Bioinformatics. 2014; 30:2114–2120. doi:10.1093/bioinformatics/btu170. [PubMed: 24695404]
38. Dobin A, et al. STAR: ultrafast universal RNA-seq aligner. Bioinformatics. 2013; 29:15–21. doi:10.1093/bioinformatics/bts635. [PubMed: 23104886]

39. Anders S, Huber W. Differential expression analysis for sequence count data. Genome biology. 2010; 11:R106. doi:10.1186/gb-2010-11-10-r106. [PubMed: 20979621]

40. Zheng Y, et al. Regulatory T-cell suppressor program co-opts transcription factor IRF4 to control T(H)2 responses. Nature. 2009; 458:351–356. doi:nature07674 [pii] 10.1038/nature07674. [PubMed: 19182775]

41. Chaudhry A, et al. CD4+ regulatory T cells control TH17 responses in a Stat3-dependent manner. Science. 2009; 326:986–991. doi:1172702 [pii] 10.1126/science.1172702. [PubMed: 19797626]

42. Stromnes IM, Goverman JM. Active induction of experimental allergic encephalomyelitis. Nat Protoc. 2006; 1:1810–1819. doi:nprot.2006.285 [pii] 10.1038/nprot.2006.285. [PubMed: 17487163]

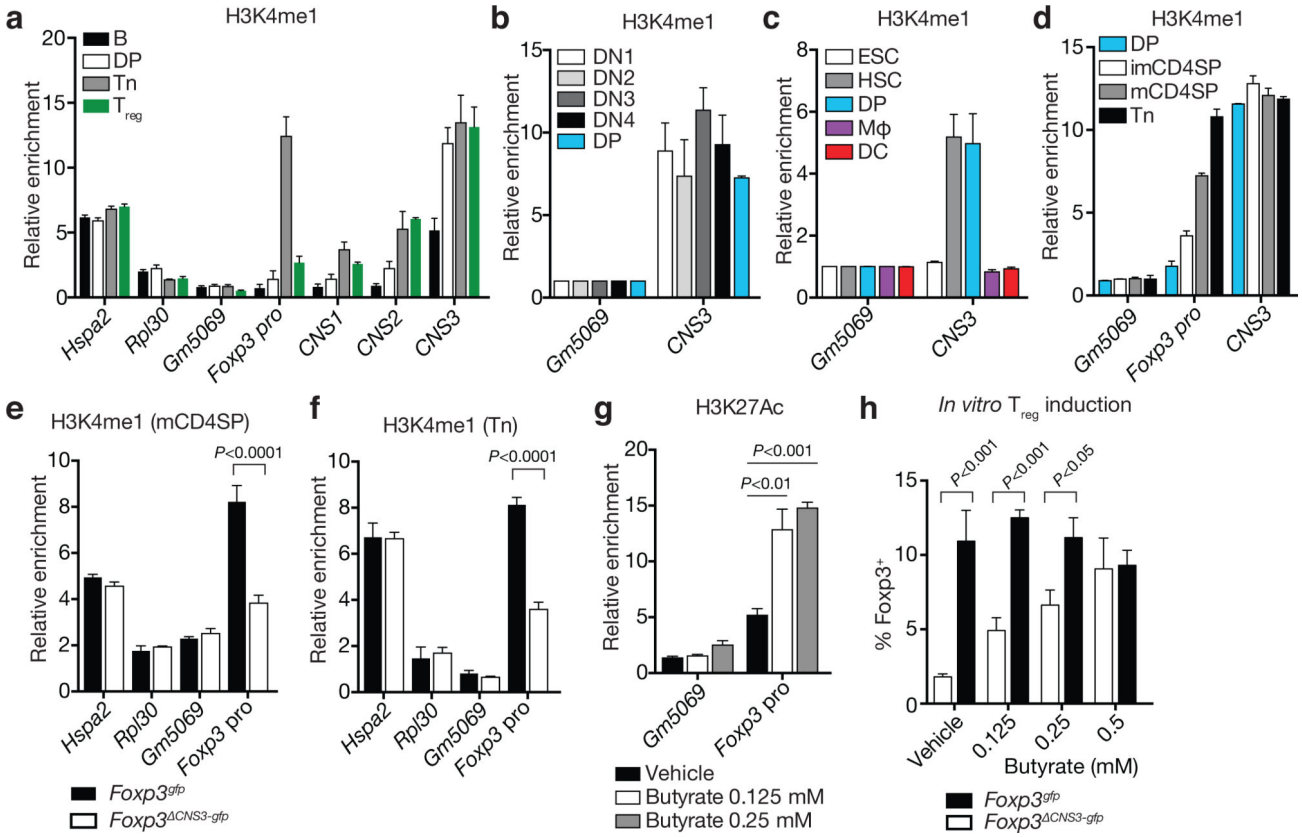

Figure 1. *CNS3* acts as an epigenetic switch for the *Foxp3* promoter poising

a, ChIP-qPCR of H3K4me1 at the *Foxp3* locus and control loci (*Hspa2*, *Rpl30* and *Gm5069*) in B cells, DP thymocytes, naïve CD4$^+$ T (Tn) and Treg cells.

b, c, H3K4me1 at *CNS3* in DN and DP thymocytes (**b**), HSC, ESC, macrophages (Mϕ) and dendritic cells (DC) (**c**).

d, H3K4me1 at the *Foxp3* promoter in DP, immature CD4 SP (imCD4SP, Foxp3$^-$CD69^{hi}CD62L^{lo}), mature CD4 SP (mCD4SP, Foxp3$^-$CD69^{lo}CD62L^{hi}) thymocytes, and naïve CD4$^+$ T cells.

e, f, *CNS3* dependent H3K4me1 at the *Foxp3* promoter in mature CD4 SP thymocytes (**e**) and naïve CD4$^+$ T cells (**f**).

g, h, HDAC inhibitor butyrate enhances H3K27Ac at the *Foxp3* promoter (**g**) and rescues impaired Treg differentiation of *CNS3*-deficient T cells *in vitro* (**h**).

Two-tailed unpaired t-test. Mean ± SEMs, represent triplicate cultures in one of ≥ 2 experiments.

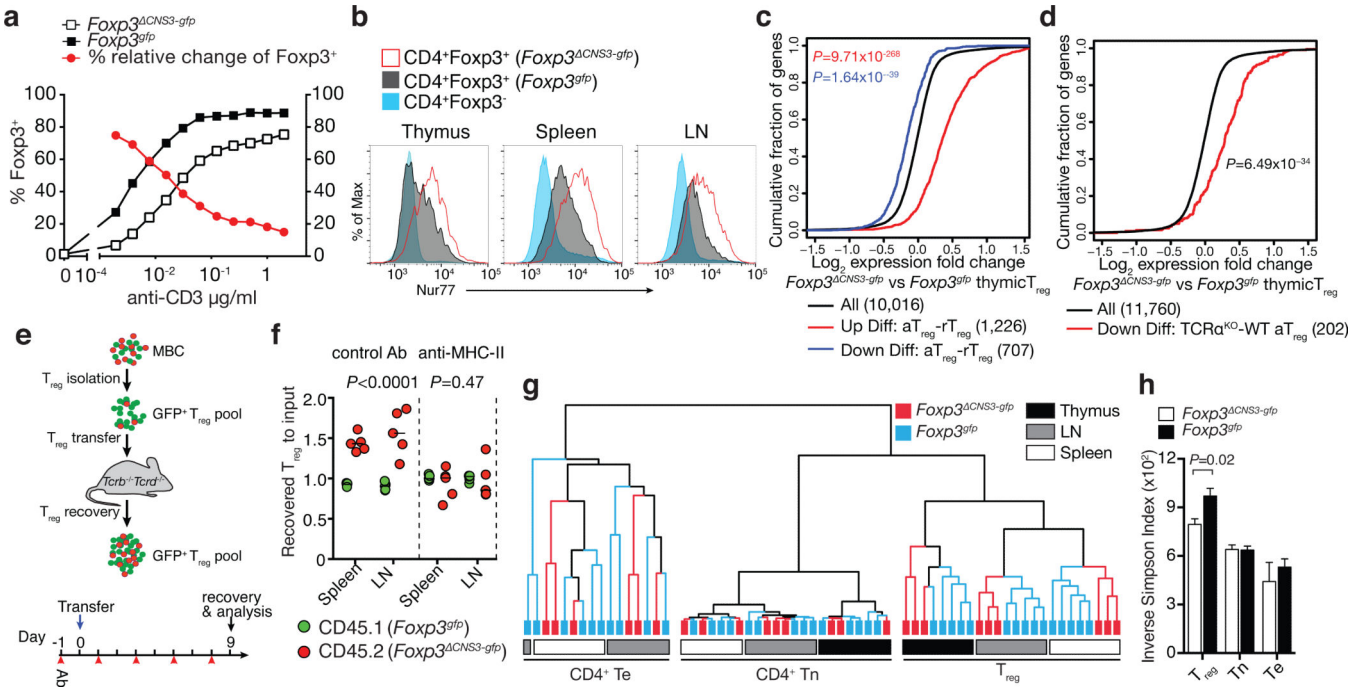

Figure 2. *CNS3* shapes the Treg cell repertoire

a, *CNS3* facilitates *in vitro* Treg induction at suboptimal TCR signaling strength. Means ± SEMs of triplicate cultures, represent one of >2 experiments.

b, Nur77 protein expression in *CNS3*-deficient and -sufficient Treg cells (Summarized in Extended Data Fig. 4b).

c, d, Relative gene expression levels (RNA-seq) were compared to the up- (Up Diff) and down-regulated (Down Diff) genes in activated (aTreg) vs. resting Treg cells (rTreg) from wild type *Foxp3*^{gfp} mice (**c**), or to those down-regulated in aTreg cells subjected to Cre-induced TCR ablation or mock treatment (**d**). The numbers of genes in each comparison are indicated in parentheses. n=3 *Foxp3*^{gfp}, n=4 *Foxp3*$^{\Delta CNS3\text{-}gfp}$. One-tailed Kolmogorov-Smirnov test.

e, f, Analysis of the expansion potentials of *CNS3*-deficient and -sufficient Treg cells in lymphopenic hosts. CD45.1 and CD45.2 Treg cells sorted from mixed bone marrow chimeras (MBC) of CD45.1 *Foxp3*^{gfp} and CD45.2 *Foxp3*$^{\Delta CNS3\text{-}gfp}$ were mixed at a 1:1 ratio and co-transferred with wild type naïve Foxp3^{-}CD4^{+} T cells into *Tcrb*$^{-/-}$*Tcrd*$^{-/-}$ recipients treated with MHC-II blocking antibody or control IgG before and after the transfer (n=5 per group). Ratios of recovered Treg cells to their inputs were shown. Two-tailed unpaired Mann Whitney test, represent one of three experiments.

g, h, Cluster (**g**) and diversity (**h**) analysis of TCRα repertoires in *Foxp3*^{gfp} (n=5) and *Foxp3*$^{\Delta CNS3\text{-}gfp}$ (n=3) *Tcra*$^{-/+}$ mice bearing DO11.10 TCRβ transgene. Identical sampling size was used to assess the diversity with the inverse Simpson index. Colored bars represent individual mice. Te, effector CD4^{+}. Means ± SEMs. Two-tailed unpaired t-test.

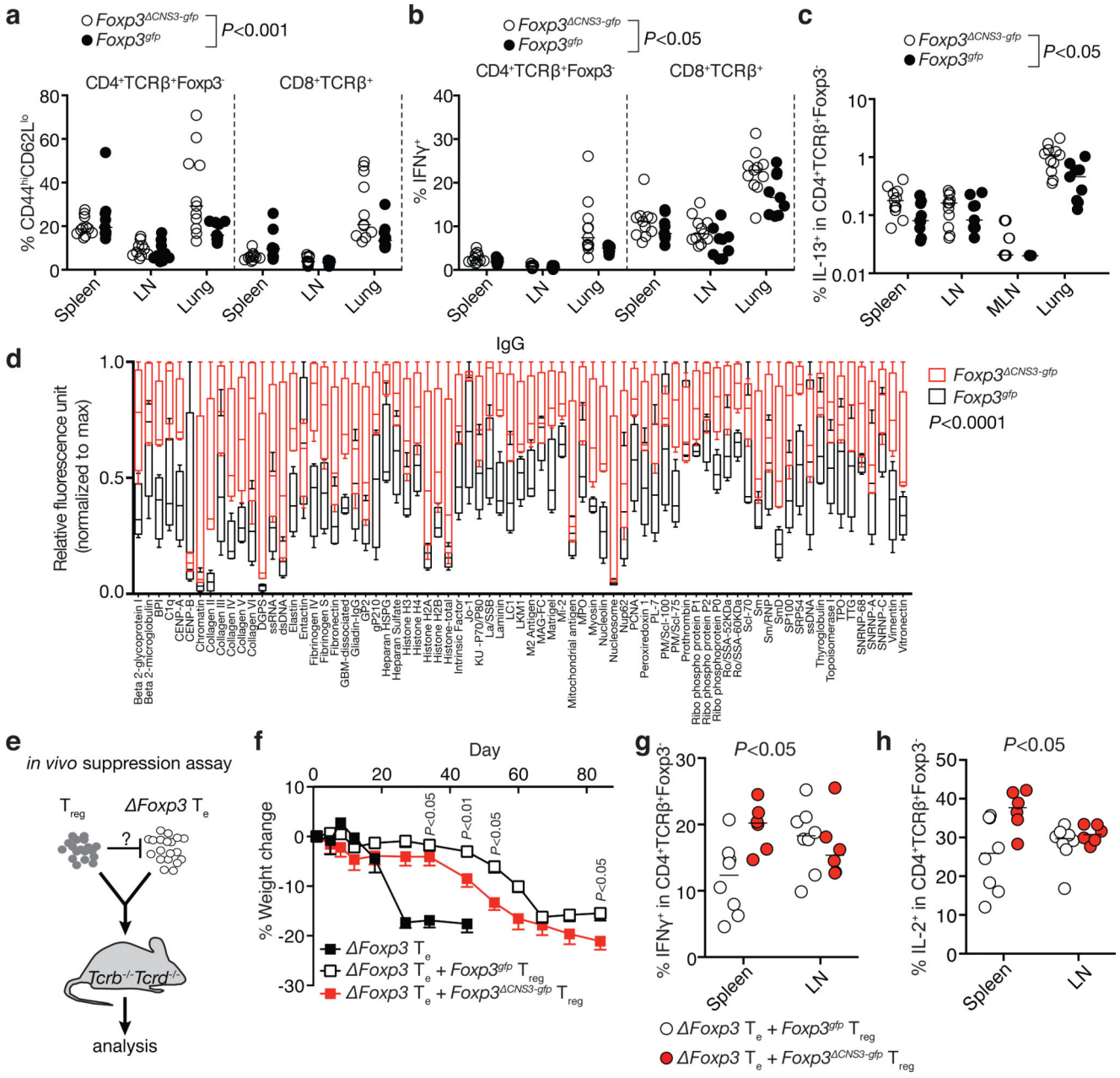

Figure 3. Defective self-tolerance in the presence of *CNS3*-deficient Treg cells

a-c, Analysis of the activation ($CD44^{hi}CD62L^{lo}$) (**a**), IFNγ (**b**) and IL-13 (**c**) production in $CD4^+Foxp3^-$ and/or $CD8^+$ T cells in *Foxp3*$^{\Delta CNS3\text{-}gfp}$ (n=11) and *Foxp3*^{gfp} mice (n=9). Two-tailed unpaired Mann Whitney tests.

d, Analysis of circulating IgG against multiple self-antigens in the serum of *Foxp3*^{gfp} and *Foxp3*$^{\Delta CNS3\text{-}gfp}$ littermates (n=4 per group). Plots show minimum, maximum, first and third quartiles and median. Two-way ANOVA.

e-h, Compromised suppressor capacity of *CNS3*-deficient Treg cells *in vivo*. $CD45.2^+$ *CNS3*-sufficient or -deficient Treg cells were co-transferred at a 1:10 ratio with CD45.1 *Foxp3*^{null} effector $CD4^+$ T cells (*ΔFoxp3* Te) into *Tcrb*$^{-/-}$*Tcrd*$^{-/-}$ mice (**e**). Recipient mice

were monitored for body weight change (**f**), IFNγ and IL-2 production (**g, h**). Mice transferred with *ΔFoxp3* Te alone succumbed to severe inflammation and were sacrificed on day 45. *ΔFoxp3* Te (n=5), *ΔFoxp3* Te + *Foxp3*^{gfp} (n=8), *ΔFoxp3* Te + *Foxp3*$^{\Delta CNS3\text{-}gfp}$ (n=6). Two-tail unpaired t-test (**f**) or Mann Whitney test (**g**-**h**). Means - SEMs (**f**). Represent two independent experiments.

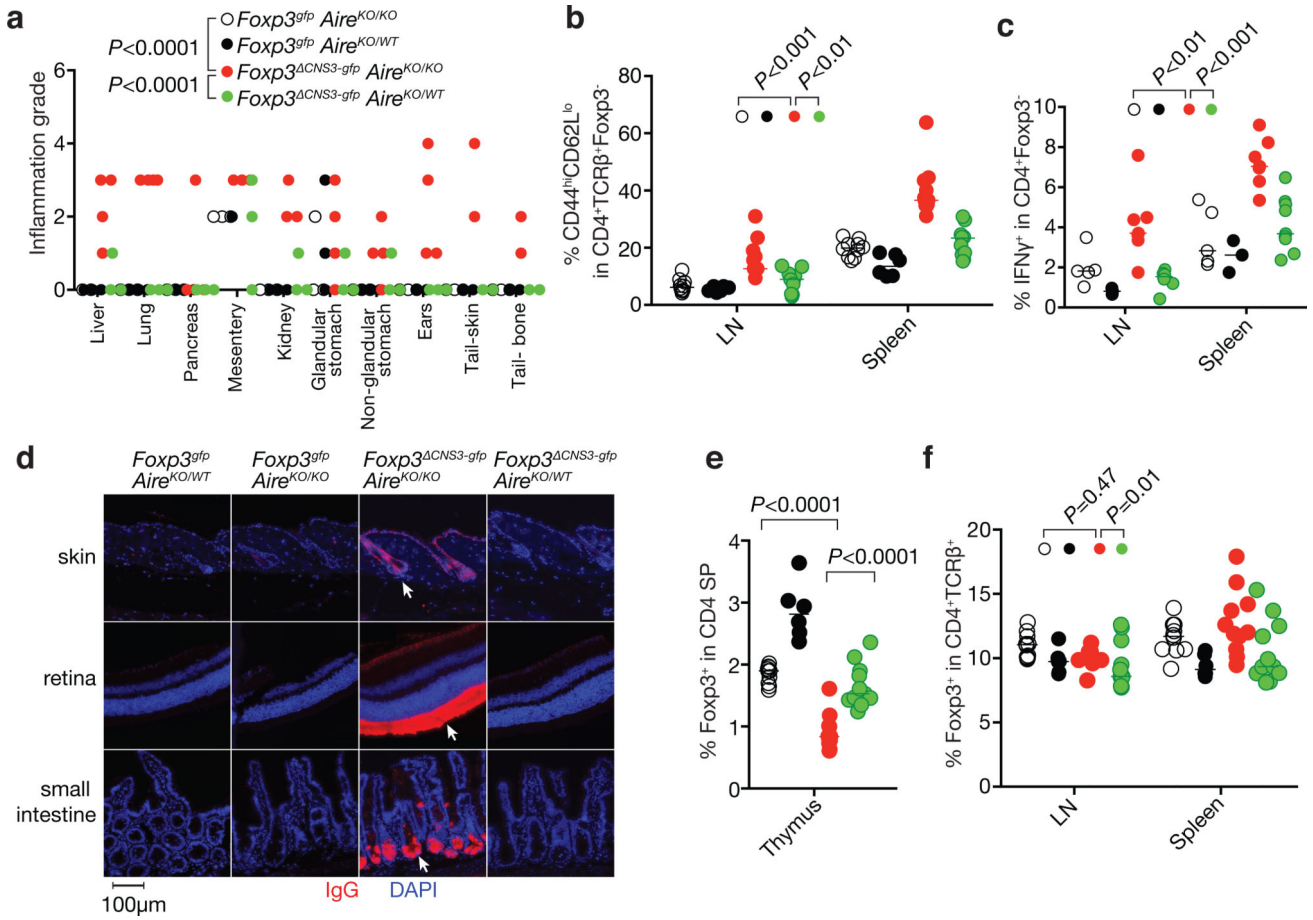

Figure 4. *CNS3*-deficient Treg cells fail to maintain self-tolerance in the absence of *Aire*

a, Analysis of tissue inflammation in *CNS3 Aire* DKO mice. n=3 per group except for *Foxp3*$^{\Delta CNS3\text{-}gfp}$ *Aire*$^{KO/KO}$ (n=4). Two-tailed unpaired Mann Whitney test.

b, Analysis of activated CD4^{+} Te cells in DKO mice. *Foxp3*^{gfp} *Aire*$^{KO/KO}$ (n=10), *Foxp3*^{gfp} *Aire*$^{KO/WT}$ (n=6), *Foxp3*$^{\Delta CNS3\text{-}gfp}$ *Aire*$^{KO/KO}$ (n=11), *Foxp3*$^{\Delta CNS3\text{-}gfp}$ *Aire*$^{KO/WT}$ (n=11). Two-tailed unpaired Mann Whitney test.

c, Analysis of IFNγ production by CD4^{+}Foxp3^{-} T cells in DKO mice. *Foxp3*^{gfp} *Aire*$^{KO/KO}$ (n=5), *Foxp3*^{gfp}*Aire*$^{KO/WT}$ (n=3), *Foxp3*$^{\Delta CNS3\text{-}gfp}$ *Aire*$^{KO/KO}$ (n=7), *Foxp3*$^{\Delta CNS3\text{-}gfp}$ *Aire*$^{KO/WT}$ (n=9). Represent >2 experiments. Two-tailed unpaired Mann Whitney test.

d, Analysis of tissue-specific autoantibodies in the serum of DKO mice. Sections of skin, intestine, and eye from gender-matched *Rag1*-deficient mice were stained with serum IgG (>8 mice per group).

e-f, Analysis of Foxp3^{+} CD4 SP thymocytes (**e**), and peripheral Treg cells in *Foxp3*$^{\Delta CNS3\text{-}gfp}$ *Aire*$^{KO/KO}$ mice (**f**). *Foxp3*^{gfp} *Aire*$^{KO/KO}$ (n=10), *Foxp3*^{gfp} *Aire*$^{KO/WT}$ (n=6), *Foxp3*$^{\Delta CNS3\text{-}gfp}$ *Aire*$^{KO/KO}$ (n=11), *Foxp3*$^{\Delta CNS3\text{-}gfp}$ *Aire*$^{KO/WT}$ (n=11). Two-tailed unpaired Mann Whitney test.